Origin and cross-century dynamics of an avian hybrid zone

Andrea Morales-Rozo[1,5]
Email: amoralesrozo@unillanos.edu.co

Elkin A. Tenorio[1,2]
Email: ek.tenorio@gmail.com

Matthew D. Carling[3,4]
Email: mcarling@uwyo.edu

Carlos Daniel Cadena[1*]
*Corresponding autor
Email: ccadena@uniandes.edu.co

[1]Laboratorio de Biología Evolutiva de Vertebrados, Departamento de Ciencias Biológicas, Universidad de Los Andes, Bogotá, Colombia

[2]Calima: Fundación para la Investigación de la Biodiversidad y Conservación en el Trópico, Cali, Colombia.

[3]Cornell Laboratory of Ornithology, Cornell University, Ithaca, NY, USA

[4]Department of Zoology and Physiology, University of Wyoming, Laramie, WY, USA

[5]Programa de Biología y Museo de Historia Natural, Universidad de los Llanos, Sede Barcelona, Villavicencio, Colombia

1   **Abstract**

2

3   **Background:** Characterizations of the dynamics of hybrid zones in space and time can give insights

4   about traits and processes important in population divergence and speciation. We characterized a

5   hybrid zone between tanagers in the genus *Ramphocelus* (Aves, Thraupidae) located in southwestern

6   Colombia. We tested whether this hybrid zone originated as a result of secondary contact or of

7   primary differentiation, and described its dynamics across time using spatial analyses of molecular,

8   morphological, and coloration data in combination with paleodistribution modeling.

9   **Results:** Models of potential historical distributions based on climatic data and genetic signatures of

10   demographic expansion suggested that the hybrid zone likely originated following secondary contact

11   between populations that expanded their ranges out of isolated areas in the Quaternary. Concordant

12   patterns of variation in phenotypic characters across the hybrid zone and its narrow extent are

13   suggestive of a tension zone, maintained by a balance between dispersal and selection against hybrids.

14   Estimates of phenotypic cline parameters obtained using specimens collected over nearly a century

15   revealed that, in recent decades, the zone appears to have moved to the east and to higher elevations,

16   and has apparently become narrower. Genetic variation was not clearly structured along the hybrid

17   zone, but comparisons between historical and contemporary specimens suggested that temporal

18   changes in its genetic makeup may also have occurred.

19   **Conclusions:** Our data suggest that the hybrid zone likey resulted from secondary contact between

20   populations. The observed changes in the hybrid zone may be a result of sexual selection, asymmetric

21   gene flow, or environmental change.

22

23   **Keywords:** Andes, cline, Hill function, distribution modeling, hybridization, moving hybrid zone.

24

Background

Characterizations of hybrid zones allow one to make inferences about traits and processes relevant to understanding the origin and maintenance of differences between populations and species [1,2]. A classic question about hybrid zones is how are they formed, with previous studies proposing two main hypotheses (reviewed by [3]). The hypothesis of secondary contact posits that hybrid zones result from expansion of populations that were previously isolated geographically and which interbreed in contact zones because complete reproductive isolation between them was not reached during the allopatric phase [4]. An alternative hypothesis postulates that hybrid zones form in parapatry, by primary differentiation across ecological gradients [5]. Secondary contact is likely if environments that presently allow the distributions of hybridizing populations to overlap were disjunct in the past, a scenario that predicts one should observe genetic signatures of population expansions. Alternatively, primary differentiation along a gradient would occur if the extent of suitable environments for the hybridizing populations has been stable over time; this predicts that populations have not expanded their ranges historically, and that the position of the hybrid zone (as indicated by the position of clines in molecular and morphological traits) is coincident with an environmental transition [1,6].

Inferring hybrid-zone origins from current patterns of variation is challenging because, with time, genetic signatures of secondary contact or primary intergradation tend to erode [3,7]. Alternatively, then, tests of hypotheses posed to account for the origin of hybrid zones may be conducted by examining the historical distribution of hybridizing taxa using paleodistributional modeling, i.e. projecting ecological niche models, which characterize the current distribution of species in climatic space, onto models of historical climatic conditions to infer potential distributions in the past [8,9]. Such models of historical distributions represent hypotheses one can further test using molecular data to evaluate their population-genetic predictions, such as signatures of population growth for presumably expanding populations and of constant population size and isolation by distance in populations occurring within climatically stable areas [10,11]. This approach has revealed that several hybrid zones likely originated following range expansions leading to secondary contact [12-15].

Another focus of studies on hybrid zones is the analysis of their temporal dynamics, which can allow understanding the role played by different evolutionary forces in such scenarios. When hybrid genotypes are less fit than parental genotypes, 'tension zones' are formed, which are maintained by a balance between the homogenizing effect of dispersal into the hybrid zone and the diversifying effect of selection against hybrids [1]. If there is endogenous selection against hybrids, then there should be coincidence in location and concordance in width of clines describing the variation in different traits and loci across a hybrid zone, and such clines should remain stable over time [16,17]. However, hybrid zones are often temporally dynamic (i.e. they may shift in location or change in width) and

62 because clines for different traits may change in different ways, one can make inferences about the

63 action of particular processes (e.g., natural selection, sexual selection, competition, asymmetric

64 hybridization, dominance drive) based on dynamics observed for different characters [18]. For

65 example, discordant patterns of plumage and mitochondrial DNA variation across a hybrid zone

66 between *Setophaga* warblers, coupled with behavioral experiments showing aggressive superiority of

67 males of one species over the other, indicate that movement of this zone has likely been driven by

68 competition-mediated asymmetric hybridization [19-21]. Temporal changes in the makeup of hybrid

69 zones may also reflect natural or human-mediated environmental changes [22,23].

70

71 There is ample evidence of hybridization between members of the tanager genus *Ramphocelus* (Aves,

72 Thraupidae; [24-27]), but detailed studies on hybrid zones involving species in this group are scant.

73 Here, we characterize a hybrid zone between members of this genus located in western Colombia that

74 has received little study although its existence was noted nearly a century ago [28] and was described

75 in some detail more than five decades ago [25]. In the Cauca River Valley above c. 900 m elevation,

76 one finds the larger form *flammigerus* (males are black with a scarlet rump), whereas the smaller and

77 yellow-rumped form *icteronotus* occurs along the costal plains west of the Andes extending north into

78 Costa Rica and south into northern Peru. Females and immatures are similar to their respective males,

79 but are less strongly colored. Along a c. 140 km transect running approximately northwest from the

80 city of Cali downslope along the western flank of the Cordillera Occidental, the two forms hybridize,

81 forming a gradient in coloration and body mass ([25,29]; Fig. 1 and 2). Currently, these forms are

82 considered subspecies of *Ramphocelus flammigerus* [30] because gene exchange between them

83 appears to be unrestricted, with apparently no selection against hybrids [25].

84

85 The *R. flammigerus* system is particularly well suited to studying the role of different evolutionary

86 forces at work in hybrid zones owing to the existence of variation in characters with different modes

87 of inheritance, and, presumably, under different forms of selection. Variation in rump coloration

88 across the hybrid zone likely reflects variation in the concentration of a single carotenoid pigment and

89 is influenced by the environment because carotenoids are obtained from the diet [25,31,32].

90 Furthermore, based on the strong sexual dichromatism in this species, and the likelihood that its

91 mating system involves some degree of polygamy [33], plumage coloration is probably influenced by

92 sexual selection. In contrast, morphometric variation [25,29] likely has a strong genetic basis [34-36]

93 and could be subject to natural selection [37-39]. The value of considering traits with different modes

94 of inheritance and under different selective pressures to understand evolutionary forces at work in

95 hybrid zones is illustrated by studies showing (1) that clines for traits involved in courtship are

96 displaced with respect to clines for presumably neutral traits or loci, suggesting a role for sexual

97 selection driving introgression [40,41]; (2) that sex-linked molecular markers introgress over shorter

98 distances than autosomal markers, suggesting a role for sex chromosomes in reproductive isolation

99   [42,43]; or (3) that there is more limited introgression in organellar DNA than in nuclear genes,

100   suggesting selection acts more strongly on hybrids of the heterogametic sex (Haldane's rule; [44]).

101

102   Here, we sought to evaluate whether the *Ramphocelus* hybrid zone in southwestern Colombia

103   originated as a result of secondary contact or of primary differentiation, and to examine the zone's

104   dynamics over nearly a century to make inferences about the action of different evolutionary

105   processes. To accomplish this, we (1) reconstructed the biogeographic and demographic history of the

106   hybridizing populations based on ecological niche modeling and coalescent analyses of mtDNA

107   sequence data, (2) characterized genetic, morphological and plumage variation across the hybrid zone,

108   and (3) compared spatial patterns of variation in morphometrics, plumage coloration, and genetic

109   structure between specimens collected at different times to assess changes in the position and width of

110   the hybrid zone.

111

Materials and methods

113

Samples

115   We characterized the *Ramphocelus* hybrid zone historically by examining specimens collected from

116   1894 to 1986 in the ornithological collections of the American Museum of Natural History, the

117   Cornell University Museum of Vertebrates, Universidad del Valle, and the Instituto de Ciencias

118   Naturales at Universidad Nacional de Colombia. To describe current patterns of variation, we

119   collected 73 new specimens in 2007-2010: 65 of them are from localities ranging across the hybrid

120   zone over a distance of 140 km by road connecting the cities of Cali and Buenaventura in department

121   Valle del Cauca [25]; the remaining eight are from localities distant from the hybrid zone in the

122   departments of Antioquia (3), Risaralda (3), and Cauca (2). Study skins and tissue samples are

123   deposited in the Museo de Historia Natural de la Universidad de los Andes (ANDES, Table S1). All

124   specimen localities (historical and current) were plotted and their position along a transect line that

125   best adjusted to points (estimated using a linear regression between latitude and longitude) was

126   recorded. To construct character clines, we recorded the perpendicular position of each specimen on

127   the regression line (Fig. 2; Table S1) and calculated the distance from the northwest extreme of our

128   study transect on the Pacific coast to the position of each specimen along the line.

129

Biogeographic history

131   To model potential distributions of the study taxa, we used 343 georeferenced localities obtained from

132   museum specimens and reliable field observations from Costa Rica, Panama, Colombia, Ecuador, and

133   Peru ([45]; GBIF Data Portal, C. Sánchez, pers. comm., our observations). We associated localities

134   with GIS layers for 19 climate variables at a c. 1 km resolution developed for the present (WorldClim;

135   [46]). With these data, we used a maximum entropy approach (Maxent; [47]) based on current climate

136   layers to generate models of the ecological niche and potential distribution of *flammigerus* and

137   *icteronotus* at present (localities of both forms and presumed hybrids were considered together).

138   Model performance in predicting present distributions (evaluated using receiver-operating-

139   characteristic curves; [48]) was satisfactory (see below), validating the use of this approach to infer

140   potential distributions in the past.

141

142   We projected models based on current climate data onto historical climate surfaces for 6,000 years ago

143   and for the Last Glacial Maximum (LGM; 21,000 years ago) to determine whether the distributions of

144   our study taxa were likely disjunct in the past as predicted by the secondary contact hypothesis, or

145   have likely been continuous as predicted by the primary intergradation hypothesis. This approach

146   requires assuming ecological niche conservatism and that climate represents a long-term stable

147   constraint on potential distributions. Because ecological niche models are based only on climatic data,

148   they tend to overpredict potential distributions into areas where the study species do not occur owing

149   to historical limitations to dispersal (e.g., the Amazon region in *R. flammigerus*). To reduce

150   overprediction, we cropped maps of current and historical distributions to include only areas within

151   the Andes Ecoregion [49]. Although cropping potential distributions to this region probably did not

152   remove all areas of model overprediction, it allowed for a semi-quantitative comparison of potential

153   distributions across different time periods by calculating the extent of presence areas within the

154   ecoregion. Maxent produces a continuous output ranging from zero to one describing the probability

155   of the species potentially being present at different sites. We considered a threshold of 10% omission

156   to categorize pixels as suitable or unsuitable for each of the time periods.

157

158   **Genetic characterization and demographic history**

159   We analyzed variation in DNA sequences of the cytochrome *b* mitochondrial gene for 58 of the

160   *flammigerus/icteronotus* individuals collected in Colombia from 2007 to 2010. In addition, we

161   obtained sequences for three individuals from Ecuador and two from Panama, and combined our data

162   with two sequences of *flammigerus* available in GenBank: one from Ecuador (accession U15719.1;

163   [50]) and one from Panamá (FJ799882.1; [51]; Table S1).

164

165   DNA was extracted from tissue samples or toepad samples taken from specimens using a Qiagen

166   DNeasy Tissue Kit or a phenol-chloroform method [52]. PCRs used primers H16064 and L14996 [53]

167   in 24 µl amplification reactions using the following conditions: 42ng of DNA, 0.416 mM dNTPs,

168   0.5mM of each primer, 1.042 units of 10X buffer with 1.56 mM MgCl2, 0.0246 units/ml AmpliTaq

169   DNA polymerase), and 16.5 of sterile ddH2O. Reactions began with an initial denaturation at 94°C for

170   two minutes, followed by 34 cycles of denaturation at 94°C for 30 s, annealing at 52°C for 30 s, and

171   extension at 72°C for one minute, with a final extension phase at 72°C for 7 minutes. PCR products

172   were purified with Affymetrix Exosap-IT and sequenced in both directions. Sequences were edited,

6

173   assembled and aligned using Geneious Pro 3.6.1 (http://www.geneious.com). The mean length of

174   these sequences was 988.8 bp (range 888-1008 bp).

175

176   We also analyzed mtDNA from historical toepad samples of 87 specimens collected by C. G. Sibley in

177   1956 and housed at the Cornell University Museum of Vertebrates [25]. DNA extraction and

178   amplification of these samples was carried out in a historical DNA lab, following protocols to reduce

179   the odds of contamination [54]. For these specimens, we amplified and sequenced c. 210 bp of the

180   cytochrome *b* gene (mean=209.9, range=203-210 bp).

181

182   We examined genealogical relationships among haplotypes observed in *flammigerus* and *icteronotus*

183   at present using a maximum-likelihood (ML) phylogenetic analysis employing the GAMMA model.

184   Nodal support was estimated using 1000 bootstrap replicates in RAxML, run from the RAxML

185   BlackBox Web-Server [55]. We used as outgroups sequences of *Ramphocelus carbo* (AF310048.1;

186   [56]) and *R. passerinii* (EF529965.1; [51]).

187

188   To assess potential changes in the genetic makeup of the hybrid zone over time, we examined

189   population structure separately for the 1956 specimens and for our samples collected in 2007-2010

190   (hereafter 2010 specimens) employing procedures implemented in the program ARLEQUIN v3.5 [57].

191   Based on each data set, we conducted analyses of molecular variance (AMOVAs). We divided our

192   sampling transect in three sectors of equal length: sector 1, 0 – 44 km; sector 2, 45-89 km; and sector

193   3, 90-134 km. Within each sector, we grouped individuals collected within 1km from each other in a

194   single locality. We calculated F-statistics to estimate differentiation among sectors (F_{CT}), among

195   localities within sectors (F_{SC}), and among localities among sectors (F_{ST}). This analysis allowed us to

196   examine whether there has been any change in the way in which genetic variation is distributed within

197   and among sectors; if spatial genetic structure has become eroded (e.g., if introgressive hybridization

198   has led to genetic homogenization across the transect), then one would expect an increase in genetic

199   variation existing within sectors and a decrease in that existing among sectors over time (i.e. higher

200   F_{CT} in the past than at present). To make data comparable across time periods, sequences for 2010

201   specimens were trimmed to match the 210 bp available for the 1956 specimens. As an additional way

202   to visualize potential changes in genetic structure over time, we constructed median-joining haplotype

203   networks for the 1956 and 2010 samples using the program PopART

204   (http://popart.otago.ac.nz/index.shtml).

205

206   To determine whether populations of *flammigerus* and *icteronotus* have experienced demographic

207   expansions or if these taxa have exhibited historically stable population sizes, we examined trends in

208   effective population size through time using the Extended Bayesian Skyline Plot (EBSP) method

209   implemented in Beast v1.7.4 [58] using sequence data for the 2010 specimens. Demographic

7

210 expansions are expected if the hybrid zone originated following secondary contact and stable

211 population sizes are expected if the zone originated by primary differentiation. Analyses used the

212 HKY+Γ model, which was selected as the best fit to the data according to the Bayesian Information

213 Criterion (BIC) in JModelTest v 2.1.3 [59]. We ran the analysis for 25,000,000 iterations of which the

214 first 10% were discarded as burn-in; genealogies and model parameters were sampled every 10,000

215 iterations. For time calibration we assumed a lognormal relaxed clock and a cytochrome-*b* substitution

216 rate of 2.08% divergence per million years [60]. We used the mean of the distribution of population

217 size as a prior (parameter "demographic.populationMean") calculated from a "Coalescent: constant

218 time" tree prior, run with the same parameters as above. Because this analysis assumes no genetic

219 structure within the sample, we only considered populations located between Cali and Buenaventura

220 (i.e., from the hybrid-zone transect). The skyline plot was built in R [61] with code written by

221 Valderrama *et al.* [62].

222

223 **Phenotypic characterization**

224 To characterize the hybrid zone phenotypically, we measured six morphological characters on

225 museum specimens (*n*=139 males, 83 females) with dial calipers to the nearest 0.1 mm: wing length

226 (chord of unflattened wing from bend of wing to longest primary), exposed culmen, bill depth (at the

227 base), bill width (at the base), tail length (from point of insertion of central rectrices to tip of longest

228 rectrix), and tarsus length (from the joint of tarsometatarsus and tibiotarsus to the lateral edge of last

229 undivided scute). To describe morphological variation, we reduced variation in these characters using

230 a principal components analysis (PCA).

231

232 We characterized plumage coloration based on reflectance spectra from 400 to 700 nm measured on

233 the rump of adult museum specimens (*n*=144 males, 70 females) using an Ocean Optics USB4F00243

234 Spectrometer with the SpectraSuite software (Ocean Optics). Three color measurements were

235 estimated for each reflectance spectrum based on segment classification analysis [63]: brightness, an

236 index of how much light is reflected from the sample relative to a white standard; chroma, the

237 saturation of color; and hue, which relates to the wavelength of maximum slope. These measurements

238 were calculated using R code written by Parra [64].

239

240 **Phenotypic clines and temporal dynamics**

241 To compare patterns of morphometric and plumage color variation among adult specimens collected at

242 different times in a geographical context, we defined three periods based on temporal sampling gaps:

243 prior to 1911, 1956-1986, and 2010. Hybrid zones are often studied using cline-fitting algorithms that

244 employ Bayesian or maximum-likelihood methods to estimate parameters like cline center and width

245 (e.g. HZAR [65], Analyse [66], ClineFit [67]), and are based on population genetic models. These

246 approaches typically require data from multiple individuals per sampling site to properly characterize

8

247 variation within and among localities; accordingly, individuals need to be sampled at (or assigned to) a

248 set of discrete sites. This approach is possible when large numbers of specimens are available and

249 when sampling schemes have been explicitly designed with the goal of characterizing variation in

250 space. In our case, many historical specimens were not collected with the specific purpose of

251 describing the *Ramphocelus* hybrid zone and were not sampled at the same set of sites across different

252 time periods. Instead, specimens were collected largely opportunistically at multiple localties and were

253 widely scattered across the study region, with sampling varying spatially and in terms of number of

254 individuals over time. Therefore, because our data did not readily allow us to assign individuals to

255 discrete sampling sites, we did not employ cline-fitting methods; instead, we described the variation in

256 morphometrics and plumage reflectance (i.e. chroma) across the hybrid zone in different time periods

257 using log-logistic models, commonly known as Hill functions [68]. These functions are based on a

258 sigmoidal dose-response (variable slope) model, which describes a response variable y (i.e. character

259 value in our study) as a function of an independent variable x (i.e. distance from the initial point of the

260 hybrid zone) based on a four-parameter logistic equation:

261
$$Y = C + \frac{(D + C)}{1 + \exp\left(B(\log(X) - \log(E))\right)}$$

262 Here, *D* and *C* are the Y values at the plateau's extremes (i.e. character values at each end of the

263 hybrid zone in our case), *B* is a coefficient denoting the steepness of the curve, and *E* corresponds to

264 the distance along the *X* axis where 50% of the value in *Y* is observed (also denoted ED50; [68]). We

265 used the ED50 value as an estimate of cline center, and estimated cline width as the difference

266 between the ED10 and ED90 values. We used this criterion to estimate cline width because ED10 and

267 ED90 define the values of phenotypes in the *X* axis beyond which there are no intermediate

268 individuals in morphology and color. For example, only individuals with scarlet-rump would be

269 observed in distances in *X* above ED90, whereas only yellow-rumped individuals would be observed

270 in distances below ED10. We calculated the above parameters using the *drm* and *ll.4* functions

271 implemented in the drc package for R [69].

272 Due to differences in sampling effort over the hybrid zone across time periods, we evaluated the

273 sensitivity of our estimates of cline center and width to sampling effects and calculated confidence

274 limits for these parameters based on a bootstrapping procedure. For each time period and for both

275 morphology and plumage reflectance data, we generated a bootstrap distribution of cline center and

276 width estimated from 1,000 data sets constructed by keeping sample size constant while resampling

277 individuals with replacement. Because in some cases sample size was small, bootstrapping resulted in

278 some samples in which variation was not clinal or in which estimates of cline parameters were

279 unrealistic given the geographic extent of the hybrid zone; therefore, we only retained bootstrap

280 samples in which the estimated cline center took values between 0 and 140 km. We compared

281   estimates of cline center and width across the tree time periods using analyses of variance (ANOVA)

282   and post-hoc Tukey tests treating estimates obtained in bootstrap samples as replicates. Likely due to a

283   low number of individuals with morphological data for the western extreme of the hybrid zone in

284   2010, bootstrap estimates of cline width for this time period were highly variable and unrealistic;

285   therefore, we do not report confidence limits for this parameter and did not include it in the ANOVA.

286   **Validation of Hill-function methods**

287   To validate the use of Hill functions to describe phenotypic and genetic clines and to infer cline center

288   and width parameters, we compared our estimates based on Hill functions to estimates obtained by

289   widely used cline-fitting algorithms (HZAR and Analyze) on a published data set that has been subject

290   to cline analyses, namely the molecular data of seven loci of the *Manacus* hybrid zone in Panama [40].

291   We used the published allele frequency data [40] to estimate cline centers and widths using our

292   approach and compared such estimates to published parameters [65]. Consistent estimates of

293   parameters across methods would validate our Hill-function approach as an alternative method to

294   estimate hybrid zone cline in scenarios where traditional algorithms cannot be used.

295

296   **Results**

297   **Biogeographic history**

298   A potential distribution model developed under current climatic conditions in Maxent accurately

299   predicted the present-day distributions of *flammigerus+icteronotus,* with an area under the ROC-curve

300   score of 0.987. Because this suggests that the assumption that climate limits distributions in these taxa

301   is reasonable, we projected models onto past climatic conditions to estimate the potential historical

302   distributions of *flammigerus+icteronotus* at 6,000 and 21,000 years ago.

303

304   Although our models evidently overpredict potential distributions, it is clear that the extent of suitable

305   environments for *flammigerus+icteronotus* has not been stable over time. The modeled potential range

306   of these taxa at present in the Northern Andes Ecoregion extends for c. 420,000 km^2. The predicted

307   potential distribution based on climate for 6,000 years ago was of similar size, with c. 460,000 km^2

308   (Fig. 3a). This indicates that current climatic conditions and those from 6,000 years ago were similarly

309   suitable for the presence of these taxa across the study region. Indeed, models suggest that the two

310   forms could have been in contact at that time in the current location of the hybrid zone (Fig. 3a). In

311   contrast, the predicted range during the LGM was considerably smaller than the predicted current

312   range (c. 280,000 km^2; Fig. 3b). Moreover, suitable conditions for *flammigerus+icteronotus* 21,000

313   years before present were not continuous along the Pacific slope of the Cordillera Occidental,

314   suggesting that these two forms were likely disjunct during the LGM. Thus, the hybrid zone may have

315   originated following population expansions and secondary contact as a result of climatic change since

10

316   the LGM, a possibility we address below based on patterns of genetic variation.

317

318   **Genetic characterization**

319   Overall, there was low genetic divergence between samples and genetic structure across the hybrid

320   zone and among other localities was limited. Based on the recent samples for which we obtained long

321   cytochrome *b* sequences, uncorrected mean sequence divergence within Colombia was only 0.3% (0-

322   1.1%); samples from Ecuador and Colombia were 1.6% divergent, and samples from Panama and

323   Colombia differed by only 0.4% on average. Except for a separation between samples from Ecuador

324   and Colombia, relationships among haplotypes were not clearly resolved by the ML phylogenetic

325   analysis, in which most nodes lacked bootstrap support and no clades associated with specific

326   geographic regions or with plumage coloration were identified (Fig. 4). Among the long sequences

327   (989 bp), there were 18 haplotypes with a total of 15 segregating sites in populations along our hybrid-

328   zone transect. Among the 87 individuals from 1956 analyzed (210 bp), there were six haplotypes, with

329   a total of nine segregating sites; uncorrected mean sequence divergence was only 0.4% (0-3.7%) and

330   most (69) individuals shared a common haplotype. Relationships among haplotypes were not

331   consistent with position along the hybrid zone (Fig. 4). For the same 210-bp region, there were seven

332   haplotypes with six segregating sites in the 2010 specimens; clear structure with respect to position

333   along the transect was not observed in the haplotype network (Fig. 4).

334

335   AMOVAs suggested that patterns of genetic structure across our study transect differ between

336   specimens from 1956 and 2010, with considerably greater genetic structure among sectors in the 1956

337   data (Table 1). For the historical data, F_{CT} values were marginally significant ($F_{CT} = 0.198$, $P = 0.011$),

338   indicating that a significant fraction of genetic variation (19%) was apportioned among sectors of the

339   study transect. This was not the case for the present-day data, in which no genetic structure across the

340   transect was detected ($F_{CT} = 0.213$, $P = 0.111$).

341

342   Although credibility intervals for population size in the Bayesian skyline plot were wide, this analysis

343   suggested that populations show a genetic signature of demographic expansion (Fig. 5). Constant

344   population size cannot be firmly rejected due to broad credibility intervals, but because the median

345   value of the parameter "demographic.populationSizeChanges" differed from zero (median value = 1,

346   95% highest posterior density 0-2), the evidence points in the direction of population expansion rather

347   than constant population size. This result is consistent with the hypothesis that the hybrid zone

348   originated as a result of secondary contact following expansion of populations from formerly disjunct

349   areas.

350

351   **Phenotypic characterization**

352   Reduction of morphometric variation using PCA resulted in a first component (PC1) describing body

353   size in both males and females. In both sexes, variables loading most heavily on this axis (which

354   accounted for 24.3% of the variation in males and 34.7% in females) were tail length and wing chord.

355   Thus, in the following we use PC1 as a general measurement of body size. We did not consider other

356   principal component axes (e.g., PC2, on which bill dimensions loaded heavily) in additional analyses

357   because they did not vary gradually across the hybrid zone.

358

359   Our estimates of cline parameters estimated using Hill functions were highly concordant with

360   published estimates obtained using HZAR and Analyse in *Manacus* [65], especially for cline center

361   (Table 2). Our estimates of cline width tended to differ more from published estimates, but in all cases

362   the values estimated from the Hill function were within confidence intervals estimated by the other

363   two algorithms. These results validate the use of the Hill function method to estimate cline parameters

364   as described below.

365

366   Morphological data for historical and recently collected male specimens provide evidence of clinal

367   variation in body size (i.e. PC1) along the hybrid zone, with birds from localities to the west

368   (*icteronotus*-type) being smaller than those from the east (*flammigerus*-type; Fig. 6). The Hill function

369   method estimated that the center of the morphometric cline is currently located at ca. 76.7 km (mean

370   across bootstrap replicates) from the coast extreme. The corresponding centers of the clines estimated

371   using the pre-1911 and 1956-1986 specimens were at ca. 67.7 and 73.8 km, respectively, suggesting

372   the zone has moved ca. 9 km over the past century (Table 3, Fig. 6, Fig.7, Fig. S1). Although

373   differences among periods were significant (Tukey's post-hoc test; Table 4), bootstrap estimates of

374   uncertainty around point estimates of cline centers overlapped broadly (Fig. 6G, Fig. 7).

375

376   Patterns of variation in color in space and time were similar to those observed for morphology. Of the

377   three measurements of plumage coloration, chroma showed the clearest clinal pattern of variation,

378   ranging from the yellow *icteronotus* to the redder *flammigerus* (Fig. 6). The Hill-function estimates of

379   cline centers did not differ significantly between the pre-1911 (72.9 km) and 1956-1986 (73.0 km)

380   periods, but the cline-center estimate for 2010 (76.3 km) was significantly different, suggesting a

381   displacement of around 3 km in eastward direction (Table 3, Table 4, Fig. 6H, Fig. 7, Fig. S1).

382

383   Estimates of cline width were substantially more uncertain, but also appear to differ between the

384   present and past. Cline width has declined across time, being wider in the pre-1911 (width 41.7 km)

385   than in the 1956-1986 (22.0 km) and 2010 (33.1 km) specimens (Table 3, Fig. 7). Likewise, the

386   estimated cline width in chroma at present was c. 6.7 km, but was wider in the past: 31.5 km in the

387   pre-1911 specimens and 32.4 km 1956-1986 specimens (Table 3, Fig. 7).

388

389   Because sample sizes for females were much lower than those of males and because variation among

12

390   female specimens across the hybrid zone was not clearly clinal (e.g., Fig. S2) we did not estimate cline

391   parameters for female morphology and plumage measurements. Likewise, because measurements of

392   plumage hue and brightness for males and females did not show clear clinal trends (data not shown),

393   we did not attempt to estimate cline parameters for these traits.

394

395   **Discussion**

396

397   Based on patterns of genetic variation, fossil pollen data, and ecological niche modeling, several

398   studies in the north temperate zone indicate that the origin of hybrid zones can be explained as a result

399   of population expansions from isolated refugia during the Quaternary [12,13,70]. Although a similar

400   hypothesis was proposed to account for the origin of contact zones in tropical rainforest organisms

401   [71,72], research on the origin of hybrid zones in the Neotropical region has been relatively limited

402   [73,74]. Our niche models indicate that potential distributions of *R. f. icteronotus* and *R. f.*

403   *flammigerus* were likely disjunct at the LGM (21,000 ya), but were potentially in contact by 6,000 ya.

404   This scenario is supported by the historical demography analysis based on mtDNA sequence data,

405   which indicates that populations have likely experienced significant range expansions, a pattern that

406   awaits confirmation with multilocus data (see below) that should allow for lower uncertainty in

407   estimates of population genetic parameters. Despite the broad credibility intervals around estimates of

408   population size through time, taken together with results of niche modelling, the pattern observed in

409   the skyline plot is consistent with a scenario in which forms likely diverged while isolated in each

410   flank of the Cordillera Occidental (*icteronotus* in the Pacific lowlands and *flammigerus* in the Cauca

411   Valley) and then expanded their distributions, presumably tracking the influence of Pleistocene

412   climate change on vegetation [75,76]. A recent study also suggested that historical climatic changes

413   likely promoted changes in the geographic distributions of lowland Neotropical birds which are

414   presently separated by the Andes [77]. Our data also suggest that the divergence between the

415   hybridizing *Ramphocelus* populations likely occurred in the Pleistocene, as indicated by low levels of

416   mtDNA divergence suggesting recent differentiation. However, because Quaternary climatic

417   oscillations started well before the LGM [78], it is possible that distribution ranges became disjunct

418   and reconnected repeatedly at various times throughout the Pleistocene.

419

420   In contrast to our proposed scenario suggesting the origin of the *Ramphocelus* hybrid zone may date to

421   at least 6,000 before present, Sibley [25] hypothesized that contact between *flammigerus* and

422   *icteronotus* resulted from recent anthropogenic deforestation and expansion of crops creating scrub

423   and second-growth habitats, which are favored by these tangers over dense rain forest. Although our

424   analyses suggest that climatic conditions were suitable for contact between these forms thousands of

425   years prior to human alterations in the area, it is likely that anthropogenic activities have facilitated

426   contact between them, possibly leading to an increased incidence of hybridization in recent times.

13

427

428   A recent study on a hybrid zone between *Heliconius* butterflies located in the same geographic region

429   where we studied hybridization in *Ramphocelus* also provided evidence consistent with the hypothesis

430   of origin via secondary contact [79]. Because there are additional documented cases of hybridization

431   in the same general area of southwestern Colombia (e.g., other *Heliconius* butterfiles [80], *Oophaga*

432   poison frogs [81]), work on the history of the region is necessary to better understand the origin and

433   maintenance of hybrid zones across taxa [12,15].

434

435   Our analyses are consistent with Sibley's [25] overall characterization of the *Ramphocelus* hybrid

436   zone: there is clinal variation in coloration and body size, with males exhibiting clearer trends than

437   females (see also [29]). With the caveat that uncertainty around parameter estimates is broad, two

438   main additional insights are provided by our cline analyses. First, our data consistently indicate that

439   for each period, clines for morphology and chroma are coincident (i.e., they have equal or very similar

440   centers). Second, variation in morphological PC1 and chroma followed the same trend over time: for

441   both traits, clines moved to the east a few kilometers and became narrower from the past to the

442   present.

443

444   The coincidence of cline centers for different characters and their apparent concordance in width in

445   each of the three periods is consistent with a tension-zone model. This is further supported by the

446   width estimated for character clines. Assuming that the hybrid zone originated at least 6,000 ya

447   according to climate-based models, that generation time in *Ramphocelus* is 1-2 years, and that

448   dispersal distances per generation lie somewhere between 1 and 20 km, the expected width of clines

449   under a neutral diffusion model (equations in [7,82]) would be between c. 25 km and more than 500

450   km. This is much wider than what we estimated (Table 2), which suggests some form of selection is

451   acting. Alternatively, narrow clines may be a result of a more recent origin of the hybrid zone than

452   implied by climate data. However, even if one assumes that the hybrid zone is as young as proposed

453   by Sibley [25], the estimated clines appear narrower than expected under neutral diffusion (c. 4-75

454   km). In sum, our results suggest that the *Ramphocelus* hybrid zone is likely a tension zone, maintained

455   by a balance between dispersal and a genome-wide barrier to gene flow [1]. This interpretation

456   contrasts with Sibley's [25] conclusions that "gene exchange appears to be unimpeded" and that there

457   is "no evidence of selection against the hybrids". Future studies should further evaluate our tension-

458   zone hypothesis by examining survival and mating success of intermediate phenotypes resulting from

459   hybridization relative to parental types.

460

461   That cline centers do not appear to be coincident across different periods for each of the characters

462   suggests movement of the *Ramphocelus* hybrid zone, but this interpretation needs to be tempered

463   because samples were not taken at exactly the same localities at each time period and because the

14

464   centers we estimated in some cases had wide support limits. However, our field observations indicate

465   that the current patterns of variation are, in fact, different from those described by Sibley [25].

466   Specifically, we frequently observed yellow-rumped individuals at Salado and Queremal, where

467   Sibley did not report any, and we also have occasional records of yellow-rumped individuals near

468   Cali, the eastern extreme of the transect. Thus, our quantitative analyses and field observations suggest

469   that the *icteronotus* phenotype (yellow rump and smaller body size) has indeed extended to the east.

470   Several previous studies have also reported on moving tension zones [83-85] although others

471   documented spatial stability [86,87].

472

473   A possible explanation for the concurrent movement of clines for different characters in hybrid zones

474   is competitive advantage of one phenotype mediated by aggression or by sexual selection [18]. Thus,

475   movement of the *Ramphocelus* hybrid zone may have been driven by competition or sexual selection

476   favoring the *icteronotus* phenotype. We believe it is unlikely that aggressive superiority of *icteronotus*

477   explains this pattern as shown in other studies of hybrid zones owing to its smaller body size, although

478   we note that in a *Manacus* (Pipridae) hybrid zone in Panama, the smaller *M. vitellinus* is more

479   aggressive than the larger *M. candei* [88]. Thus, it would be of interest to study mating patterns in the

480   field and to conduct mate-choice experiments to determine whether the *icteronotus* phenotype has

481   increased reproductive success as a result of sexual selection via male-male dominance or female

482   choice [89,90].

483   If sexual selection is based on carotenoid plumage color, which presumably is strongly influenced by

484   the environment [32], then it is somewhat puzzling that coloration seems to have moved across the

485   hybrid zone in concert with morphometric variation, which presumably has high heritability and is not

486   involved in mate choice. It is possible, however, that the ability to obtain, accumulate and metabolize

487   carotenoids has a heritable genetic basis [91] and that the fitness advantages it confers may be linked

488   to genes involved in reproductive isolation [92]. If this were the case in *R. flammigerus*, then it would

489   represent a plausible explanation for the movement of coloration in concert with others traits.

490

491   An alternative explanation for zone movement was proposed by Sibley [25], who predicted that the

492   *icteronotus* phenotype would introgress across the hybrid zone as a consequence of increased gene

493   flow from coastal to interior populations resulting from larger populations sizes in the former. This

494   could be studied in the future with multilocus estimates of effective population sizes and of the

495   magnitude of gene flow in both directions [93]. In addition, if deforestation has indeed resulted in

496   increases in population size as hypothesized by Sibley [25], then movement of the hybrid zone may

497   also partly reflect anthropogenic influences. Because hybrid zones tend to become entrapped in areas

498   of low population densities acting as sinks for migration [1,87], any changes in population size related

499   to habitat modification may have partly facilitated the observed movement of the *Ramphocelus* hybrid

15

500   zone.

501   We note that the inferred movement of the hybrid zone involves not only a west-east displacement, but

502   also a shift in its center to higher elevations in the Andes. Because the elevational ranges of tropical

503   birds may shift upslope in response to global warming [94], it is also possible that the movement of

504   the hybrid zone is related to climatic change over the past few decades [18,22,95,96], as recently

505   documented for hybrid zones between woodpecker (Picidae) and chickadee (Paridae) species in North

506   America [97,98].

507

508   In contrast to multiple studies on hybridization in birds finding significant mtDNA divergence

509   between populations located away from the center of hybrid zones and clinal variation in haplotype

510   frequencies across them (e.g., [40,44,54,73,86,99-103]), mtDNA variation was not geographically

511   structured in our study system, a likely consequence of recent divergence of the hybridizing

512   populations or of high levels of introgression. Because no clinal variation was observed across the

513   *Ramphocelus* hybrid zone, we were unable estimate cline parameters for different time periods to

514   examine zone movement as done in a few studies on hybrid zones examining genetic variation in

515   specimens collected at different times [23,85,101,104]. However, our analyses revealing more limited

516   genetic structure across the zone as indicated by F-statistics in 2010 relative to 1956 provide some

517   evidence that patterns of genetic variation may have not been stable over time. We hypothesize that

518   these results may reflect an increase in introgression of mtDNA across our study transect since

519   Sibley's [25] time, but we acknowledge that because we only assayed a small fragment of mtDNA and

520   because sampling was not spatially even between time periods, drawing any conclusion at this time

521   would be premature. Nonetheless, our preliminary genetic data suggest that assessing temporal

522   variation in spatial genetic structure using genome-wide markers (cf. [43]) would represent a fruitful

523   avenue to better understand the ecological and evolutionary forces at work in this moving hybrid zone.

524   Also, if shallow mtDNA divergence reflects overall patterns in neutral divergence, then the

525   *Ramphocelus* hybrid zone appears especially well-suited for analyses of variation in functionally

526   important genes, which may provide important insights about the genetic basis of phenotypic variation

527   [105,106].

528

529   Finally, our study serves to illustrate that Hill functions and bootstrap resampling are useful statistical

530   tools to characterize patterns of variation across hybrid zones. In contrast to other studies [e.g., 23],

531   our work was not systematically designed to examine changes in the structure of the *Ramphocelus*

532   hybrid zone over time, with repeated sampling of multiple specimens at fixed locations; rather,

533   specimens were collected by numerous researchers, often opportunistically, for different purposes, and

534   with no common sampling schemes at different times. Therefore, we did not feel confident in

535   assigning individuals to discrete localities as required for cline-fitting algorithms which rely on

16

536   calculating means and variances for samples of specimens from the same sites [65-67]. Our reanalysis

537   of a previously published data set suggests that cline parameters estimated using Hill functions mirror

538   closely those estimated by software commonly employed in studies of hybrid zones, suggesting such

539   functions are useful alternatives when methods designed to study clines cannot be employed due to the

540   nature of the available data. Although Hill functions have been used mainly to model dose-response

541   curves, in principle they can be used to describe any relationship between variables that follows a

542   sigmoid shape. In addition to not requiring data to be grouped in localities (i.e. each specimen

543   conserves its position along sampling transects), the approach we followed does not assume normality

544   in the data and can be run with low computational requeriments and relatively small sample sizes. On

545   the other hand, we suspected that due to variation in the spatial distribution and number of specimens

546   over time, inferences about temporal changes in the structure of the hybrid zone could be

547   compromised by unequal sampling. However, by analyzing variation in bootstrap samples of

548   specimens, we were able to account for sampling effects, finding that despite inconsistent sampling

549   over time, there is sufficient signal in our data to document temporal changes in spatial patterns of

550   phenotypic variation. Similar approaches could be employed to analyse temporal changes in spatial

551   variation in genetic or phenotypic traits in other systems in which museum specimens have not been

552   systematically collected over time and space but nonetheless contain rich historical information.

553

Conclusions

555   Models of potential historical distributions based on climatic data and genetic signatures of

556   demographic expansion suggested that the *Ramphocelus* hybrid zone we studied originated following

557   secondary contact between populations that expanded their ranges out of isolated areas in the

558   Quaternary, likely as a consequence of climatic change. Concordant patterns of variation in

559   phenotypic characters across the hybrid zone and its narrow extent are suggestive of a tension zone,

560   maintained by a balance between dispersal and selection against hybrids. In addition, our estimates of

561   phenotypic cline parameters obtained using specimens collected over nearly a century revealed that

562   the zone has moved to the east and to higher elevations, and has likely become narrower. These

563   observed changes in the hybrid zone may be a result of sexual selection, asymmetric gene flow, or

564   environmental change. Our data represent a baseline for a variety of ecological, behavioral, and

565   genetic studies that could shed further light on the forces involved in speciation and hybrid-zone

566   dynamics in this system.

567

Competing Interests

569   The authors declare they have no competing interests.

570

Authors' Contributions

572 AMR and CDC conceived the study. AMR collected and measured specimens, conducted molecular

573 genetic work, and performed initial analyses. MDC conducted molecular work on historical

574 specimens. AMR and EAT analyzed data with supervision from CDC. AMR and CDC wrote the

575 manuscript, with input from EAT and MDC. All authors read, commented on, and approved the final

576 manuscript.

577

Acknowledgments

594

References

596 1. Barton NH, Hewitt GM. Analysis of hybrid zones. Annu Rev Ecol Syst 1985;16:113–48.

597 2. Coyne JA, Orr HA. Speciation. Sunderland: Sinauer Associates; 2004.

598 3. Durrett R, Buttel L, Harrison R. Spatial models for hybrid zones. Heredity. 2000;84:9–19.

599 4. Mayr E. Systematics and the origin of species, from the viewpoint of a zoologist. Harvard
600 University Press; 1942.

601 5. Harrison RG. Hybrid zones: windows on evolutionary process. In: Futuyma DJ, Antonovics J,
602 editors. Oxford surveys in evolutionary biology. Oxford: Oxford University Press; 1990. pp. 69–128.

603 6. Vines TH, Köhler SC, Thiel M, Ghira I, Sands TR, MacCallum CJ, et al. The maintenance of
604 reproductive isolation in a mosaic hybrid zone between the fire-bellied toads *Bombina bombina* and *B.*
605 *variegata*. Evolution. 2003;57:1876–88.

606 7. Endler JA. Geographic variation, speciation, and clines. Princeton University Press; 1977.

607   8. Peterson AT, Martínez-Meyer E, González-Salazar C. Reconstructing the Pleistocene geography of
608   the *Aphelocoma* jays (Corvidae). Drivers Distrib. 2004;10:237–46.

609   9. Carstens BC, Richards CL. Integrating coalescent and ecological niche modeling in comparative
610   phylogeography. Evolution. 2007;61:1439–54.

611   10. Richards CL, Carstens BC, Knowles L. Distribution modelling and statistical phylogeography: an
612   integrative framework for generating and testing alternative biogeographical hypotheses. J Biogeog.
613   2007;34:1833–45.

614   11. Carnaval AC, Hickerson MJ, Haddad CFB, Rodrigues MT, Moritz C. Stability predicts genetic
615   diversity in the Brazilian Atlantic forest hotspot. Science. 2009;323:785–9.

616   12. Swenson NG. Gis-based niche models reveal unifying climatic mechanisms that maintain the
617   location of avian hybrid zones in a North American suture zone. J Evol Biol 2006;19:717–25.

618   13. Ruegg KC, Hijmans RJ, Moritz C. Climate change and the origin of migratory pathways in the
619   Swainson's thrush, *Catharus ustulatus*. J Biogeog. 2006;33:1172–82.

620   14. Swenson NG. The past and future influence of geographic information systems on hybrid zone,
621   phylogeographic and speciation research. J Evol Biol. 2008;21:421–34.

622   15. Moritz C, Hoskin CJ, MacKenzie JB, Phillips BL, Tonione M, Silva N, et al. Identification and
623   dynamics of a cryptic suture zone in tropical rainforest. Proc R Soc Lond B Biol Sci. 2009;276:1235–
624   44.

625   16. Moore BR, Price JT. Nature of selection in the northern flicker hybrid zone and its implications for
626   speciation theory. In: Harrison RG, editor. *Hybrid zones and the evolutionary process*. Oxford
627   University Press; 1993. pp. 196–225.

628   17. Kruuk LEB, Baird SJE, Gale KS, Barton NH. A comparison of multilocus clines maintained by
629   environmental adaptation or by selection against hybrids. Genetics. 1999;153:1959–71.

630   18. Buggs RJA. Empirical study of hybrid zone movement. Heredity. 2007;99:301–12.

631   19. Rohwer S, Bermingham E, Wood C. Plumage and mitochondrial DNA haplotype variation across
632   a moving hybrid zone. Evolution. 2001;55:405–22.

633   20. Krosby M, Rohwer S. A 2000 km genetic wake yields evidence for northern glacial refugia and
634   hybrid zone movement in a pair of songbirds. Proc R Soc Lond B Biol Sci. 2009;276:615–21.

635   21. Krosby M, Rohwer S. Ongoing movement of the Hermit warbler X Townsend's warbler hybrid
636   zone. PLoS One; 2010;5:e14164.

637   22. Taylor SA, Larson EL, Harrison RG. Hybrid zones: windows on climate change. Trends Ecol
638   Evolut. 2015;30:398–406.

639   23. Leaché AD, Grummer JA, Harris RB, Breckheimer IK. Evidence for concerted movement of
640   nuclear and mitochondrial clines in a lizard hybrid zone. Mol Ecol. 2017;23:75.

641   24. Griscom L. Notes on imaginary species of *Ramphocelus*. Auk. 1932;49:199–203.

642   25. Sibley CG. Hybridization in some colombian tangers, avian genus *Ramphocelus*. Proc Am Philos
643   Soc. 1958;102:448–53.

644   26. Olson SL, Violani C. Some unusual hybrids of *Ramphocelus*, with remarks on evolution in the

645   genus (Aves: Thraupinae). Boll Mus Regionale Sci Nat Torino. 1995;13:297–312.

646   27. McCarthy EM. Handbook of avian hybrids of the world. Oxford University Press, USA; 2006.

647   28. Chapman FM. The distribution of bird-life in Colombia; a contribution to a biological survey of
648   South America. Bull Am Mus Nat Hist. 1917;36:1–729.

649   29. Bedoya MJ, Murillo OE. Evidencia morfológica de hibridación entre las subespecies de
650   *Ramphocelus flammigerus* (Passeriformes: Thraupidae) en Colombia. Rev Biol Trop. 2012;60:75–85.

651   30. Remsen JV Jr, Areta JI, Cadena CD, Claramunt S, Jaramillo A, Pacheco JF, et al. A classification
652   of the bird species of South America. American Ornithologists' Union. 2017: Available from:
653   http://www.museum.lsu.edu/~Remsen/SACCBaseline.html

654   31. Plath K. Color change in *Ramphocelus flammigerus*. Auk. 1945;62:304.

655   32. Brush AH. Pigments in hybrid, variant and melanic tanagers (birds). Comp Biochem Physiol.
656   1970;36:785–93.

657   33. Krueger TR, Williams DA, Searcy WA. The genetic mating system of a tropical tanager. Condor.
658   2008;110:559–62.

659   34. Keller LF, Grant PR, Grant BR, Petren K. Heritability of morphological traits in Darwin's finches:
660   misidentified paternity and maternal effects. Heredity. 2001;87:325–36.

661   35. Bears H, Drever MC, Martin K. Comparative morphology of Dark-eyed juncos *Junco hyemalis*
662   breeding at two elevations: a common aviary experiment. J Avian Biol. 2008;39:152–62.

663   36. Ballentine B, Greenberg R. Common garden experiment reveals genetic control of phenotypic
664   divergence between swamp sparrow subspecies that lack divergence in neutral genotypes. PLoS One.
665   2010;5:e10229.

666   37. Schluter D, Smith JNM. Natural selection on beak and body size in the song sparrow. Evolution.
667   1986;40:221–31.

668   38. Grant PR, Grant BR. Unpredictable evolution in a 30-year study of Darwin's finches. Science.
669   2002;296:707–11.

670   39. Benkman CW. Divergent selection drives the adaptive radiation of crossbills. Evolution.
671   2003;57:1176–81.

672   40. Brumfield RT, Jernigan RW, McDonald DB, Braun MJ. Evolutionary implications of divergent
673   clines in an avian (Manacus: Aves) hybrid zone. Evolution. 2001;55:2070–87.

674   41. Baldassarre DT, White TA, Karubian J, Webster MS. Genomic and morphological analysis of a
675   semipermeable avian hybrid zone suggests asymmetrical introgression of a sexual signal. Evolution.
676   2014;68:2644–57.

677   42. Carling MD, Brumfield RT. Speciation in *Passerina* buntings: introgression patterns of sex-linked
678   loci identify a candidate gene region for reproductive isolation. Mol Ecol. 2009;18:834–47.

679   43. Taylor SA, Curry RL, White TA, Ferretti V, Lovette IJ. Spatiotemporally consistent genomic
680   signatures of reproductive isolation in a moving hybrid zone. Evolution. 2014;68:3066–81.

681   44. Gowen FC, Maley JM, Cicero C, Peterson AT, Faircloth BC, Warr TC, et al. Speciation in
682   Western Scrub-Jays, Haldane's rule, and genetic clines in secondary contact. BMC Evol Biol.

683   2014;14:135.

684   45. Darwin Database. BIOMAP Alliance Partners. 2007: Available from:
685   http://www.biomap.net/BioMAP/login_en.php

686   46. Hijmans RJ, Cameron SE, Parra JL, Jones PG, Jarvis A. Very high resolution interpolated climate
687   surfaces for global land areas. Int J Climatol. 2005;25:1965–78.

688   47. Phillips SJ, Anderson RP, Schapire RE. Maximum entropy modeling of species geographic
689   distributions. Ecol Modell. 2006;190:231–59.

690   48. Fielding AH, Bell JF. A review of methods for the assessment of prediction errors in conservation
691   presence/absence models. Environ Conserv. 1997;24:38–49.

692   49. Dinerstein E. A conservation assessment of the terrestrial ecoregions of Latin America and the
693   Caribbean. Washington, D.C.: World Bank; 1995.

694   50. Hackett SJ. Molecular phylogenetics and biogeography of tanagers in the genus *Ramphocelus*
695   (Aves). Mol Phylogenet Evol. 1996;5:368–82.

696   51. Burns KJ, Racicot RA. Molecular phylogenetics of a clade of lowland tanagers: implications for
697   avian participation in the Great American Interchange. Auk. 2009;126:635–48.

698   52. Sambrook J, Russell DW. Molecular cloning: a laboratory manual. Third Edition. Cold Spring
699   Harbor, N.Y.: Cold Spring Harbor Laboratory; 2001.

700   53. Sorenson MD, Ast JC, Dimcheff DE, Yuri T, Mindell DP. Primers for a PCR-based approach to
701   mitochondrial genome sequencing in birds and other vertebrates. Mol Phylogenet and Evol.
702   1999;12:105–14.

703   54. Carling MD, Serene LG, Lovette IJ. Using historical DNA to characterize hybridization between
704   Baltimore Orioles (*Icterus galbula*) and Bullock's Orioles (*I. bullockii*). Auk. 2011;128:61–8.

705   55. Stamatakis A, Hoover P, Rougemont J. A rapid bootstrap algorithm for the RAxML Web servers.
706   Syst Biol. 2008;57:758–71.

707   56. Sato A, Tichy H, O'hUigin C, Grant PR, Grant BR, Klein J. On the origin of Darwin's finches. Mol
708   Biol Evol. 2001;18:299–311.

709   57. Excoffier L, Lischer HEL. Arlequin suite ver 3.5: a new series of programs to perform population
710   genetics analyses under Linux and Windows. Mol Ecol Resour. 2010;10:564–7.

711   58. Heled J, Drummond AJ. Bayesian inference of population size history from multiple loci. BMC
712   Evol Biol. 2008;8:289.

713   59. Darriba D, Taboada GL, Doallo R, Posada D. jModelTest 2: more models, new heuristics and
714   parallel computing. Nat Methods. 2012;9:772.

715   60. Weir JT, Price M. Andean uplift promotes lowland speciation through vicariance and dispersal in
716   *Dendrocincla* woodcreepers. Mol Ecol. 2011;20:4550–63.

717   61. R Development Core Team. R: A language and environment for statistical computing. R
718   Foundation for Statistical Computing, Vienna, Austria. URL http://www.R-project.org/. 2013.

719   62. Valderrama E, Pérez-Emán JL, Brumfield RT, Cuervo AM, Cadena CD. The influence of the
720   complex topography and dynamic history of the montane Neotropics on the evolutionary

721 differentiation of a cloud forest bird (*Premnoplex brunnescens*, Furnariidae). J Biogeog.
722 2014;41:1533–46.

723 63. Endler JA. On the measurement and classification of colour in studies of animal colour patterns.
724 Biol J Linn Soc. 1990;41:315–52.

725 64. Parra JL. Color evolution in the hummingbird genus *Coeligena*. Evolution. 2009;64:324–35.

726 65. Derryberry EP, Derryberry GE, Maley JM, Brumfield RT. HZAR: hybrid zone analysis using an R
727 software package. Mol Ecol Resour. 2014;14:652–63.

728 66. Barton NH, Baird S. Analyse: software for the analysis of geographic variation and hybrid zones.
729 University of Edinburgh; 1999.

730 67. Porter AH, Wenger R, Geiger H, Scholl A, Shapiro AM. The *Pontia daplidice-edusa* hybrid zone
731 in northwestern Italy. Evolution. 1997;51:1561–73.

732 68. Ritz C, Baty F, Streibig JC, Gerhard D. Dose-Response Analysis Using R. PLoS One.
733 2015;10:e0146021.

734 69. Ritz C, Streibig JC. Bioassay analysis using R. J Stat Softw. 2005;12:1–22.

735 70. Hewitt G. The genetic legacy of the Quaternary ice ages. Nature. 2000;405:907–13.

736 71. Haffer J. Speciation in colombian forest birds west of the Andes. Am Mus Novit. 1967;2294:1–57.

737 72. Endler JA. Problems in distinguishing historical from ecological factors in biogeography. Am
738 Zool. 1982;22:441–52.

739 73. Brumfield RT. Mitochondrial variation in bolivian populations of the Variable Antshrike
740 (*Thamnophilus caerulescens*). Auk. 2005;122:414–32.

741 74. Dasmahapatra KK, Lamas G, Simpson F, Mallet J. The anatomy of a "suture zone" in Amazonian
742 butterflies: a coalescent- based test for vicariant geographic divergence and speciation. Mol Ecol.
743 2010;19:4283–301.

744 75. Hooghiemstra H, Van der Hammen T. Quaternary Ice-Age dynamics in the Colombian Andes:
745 developing an understanding of our legacy. Philos Trans R Soc Lond Biol Sci. 2004;359:173–81.

746 76. Ramírez-Barahona S, Eguiarte LE. The role of glacial cycles in promoting genetic diversity in the
747 Neotropics: the case of cloud forests during the Last Glacial Maximum. Ecol Evol. 2013;3:725–38.

748 77. Cadena CD, Pedraza CA, Brumfield RT. Climate, habitat associations and the potential
749 distributions of Neotropical birds: Implications for diversification across the Andes. Rev Acad
750 Colomb Cienc Ex Fis Nat 2016;40:275.

751 78. Jansson R, Dynesius M. The fate of clades in a world of recurrent climatic change: Milankovitch
752 oscillations and evolution. Annu Rev Ecol Syst 2002;33:741–77.

753 79. Arias CF, Rosales C, Salazar C, Castaño J, Bermingham E, Linares M, et al. Sharp genetic
754 discontinuity across a unimodal *Heliconius* hybrid zone. Mol Ecol. 2012;21:5778–94.

755 80. Arias CF, Muñoz AG, Jiggins CD, Mavárez J, Bermingham E, Linares M. A hybrid zone provides
756 evidence for incipient ecological speciation in Heliconius butterflies. Mol Ecol. 2008;17:4699–712.

757 81. Medina I, Wang IJ, Salazar C, Amézquita A. Hybridization promotes color polymorphism in the

758   aposematic harlequin poison frog, *Oophaga histrionica*. Ecol Evol. 2013;3:4388–400.

759   82. Barton NH, Gale KS. Genetic analysis of hybrid zones. In: Harrison RG, editor. Hybrid zones and
760   the evolutionary process. New York: Oxford Univ. Press; 1993. pp. 13–45.

761   83. Gay L, Crochet P-A, Bell DA, Lenormand T. Comparing clines on molecular and phenotypic traits
762   in hybrid zones: a window on tension zone models. Evolution. 2008;62:2789–806.

763   84. Dasmahapatra KK, Blum MJ, Aiello A, Hackwel S, Davies N, Bermingham EP, et al. Inferences
764   from a rapidly moving hybrid zone. Evolution. 2002;56:741–53.

765   85. Smith KL, Hale JM, Gay L, Kearney M, Austin JJ, Parris KM, et al. Spatio-temporal changes in
766   the structure of an Australian frog hybrid zone: a 40-year perspective. Evolution. 2013;67:3442–54.

767   86. Mettler RD, Spellman GM. A hybrid zone revisited: molecular and morphological analysis of the
768   maintenance, movement, and evolution of a Great Plains avian (Cardinalidae: *Pheucticus*) hybrid
769   zone. Mol Ecol. 2009;18:3256–67.

770   87. Rosser N, Dasmahapatra KK, Mallet J. Stable *Heliconius* butterfly hybrid zones are correlated
771   with a local rainfall peak at the edge of the Amazon basin. Evolution. 2014;68:3470–84.

772   88. McDonald DB, Clay RP, Brumfield RT, Braun MJ. Sexual selection on plumage and behavior in
773   an avian hybrid zone: experimental tests of male-male interactions. Evolution. 2001;55:1443–51.

774   89. Bronson CL, Grubb TCJ, Sattler DG, Braun MJ. Mate preference: a possible causal mechanism for
775   a moving hybrid zone. Anim Behav. 2003;65:489–500.

776   90. Stein AC, Uy JAC. Unidirectional introgression of a sexually selected trait across an avian hybrid
777   zone: a role for female choice? Evolution. 2006;60:1476–85.

778   91. Toews DPL, Hofmeister NR, Taylor SA. The evolution and genetics of carotenoid processing in
779   animals. Trends Genet. 2017;33:171–82.

780   92. Blount JD, McGraw KJ. Signal functions of carotenoid coloration. In: Britton G, Liaaen-Jensen S,
781   editors. Carotenoids. Basel: Birkhauser; 2008. pp. 213–36.

782   93. Hey J. Multilocus methods for estimating population sizes, migration rates and divergence time,
783   with applications to the divergence of *Drosophila pseudoobscura* and *D. persimilis*. Genetics.
784   2004;167:747–60.

785   94. Jankowski JE, Londoño GA, Robinson SK, Chappell MA. Exploring the role of physiology and
786   biotic interactions in determining elevational ranges of tropical animals. Ecography. 2012;36:1–12.

787   95. Engler JO, Rödder D, Elle O, Hochkirch A, Secondi J. Species distribution models contribute to
788   determine the effect of climate and interspecific interactions in moving hybrid zones. J Evol Biol.
789   2013;26:2487–96.

790   96. Chunco AJ. Hybridization in a warmer world. Ecol Evol. 2014;4:2019–31.

791   97. Billerman SM, Murphy MA, Carling MD. Changing climate mediates sapsucker (Aves:
792   Sphyrapicus) hybrid zone movement. Ecol Evol. 2016;6:7976–90.

793   98. Taylor SA, White TA, Hochachka WM, Ferretti V, Curry RL, Lovette IJ. Climate-mediated
794   movement of an avian hybrid zone. Curr Biol. 2014;24:671–6.

795   99. Parsons TJ, Olson SL, Braun MJ. Unidirectional spread of secondary sexual plumage traits across

23

796   an avian hybrid zone. Science. 1993;260:1643–6.

797   100. Ruegg KC. Genetic, morphological, and ecological characterization of a hybrid zone that spans a
798   migratory divide. Evolution. 2008;62:452–66.

799   101. Carling MD, Zuckerberg B. Spatio-temporal changes in the genetic structure of the *Passerina*
800   bunting hybrid zone. Mol Ecol. 2011;20:1166–75.

801   102. Milá B, Toews DPL, Smith BT, Wayne RK. A cryptic contact zone between divergent
802   mitochondrial DNA lineages in southwestern North America supports past introgressive hybridization
803   in the yellow- rumped warbler complex (Aves: *Dendroica coronata*). Biol J Linn Soc. 2011;103:696–
804   706.

805   103. Miller MJ, Lipshutz SE, Smith NG, Bermingham E. Genetic and phenotypic characterization of a
806   hybrid zone between polyandrous Northern and Wattled Jacanas in Western Panama. BMC Evol Biol.
807   2014;14:227.

808   104. Engebretsen KN, Barrow LN, Rittmeyer EN, Brown JM, Moriarty Lemmon E. Quantifying the
809   spatiotemporal dynamics in a chorus frog (Pseudacris) hybrid zone over 30 years. Ecol Evol.
810   2016;6:5013–31.

811   105. Poelstra JW, Vijay N, Bossu CM, Lantz H, Ryll B, Müller I, et al. The genomic landscape
812   underlying phenotypic integrity in the face of gene flow in crows. Science. 2014;344:1410–4.

813   106. Toews DPL, Taylor SA, Vallender R, Brelsford A, Butcher BG, Messer PW, et al. Plumage
814   genes and little else distinguish the genomes of hybridizing warblers. Curr. Biol. 2016;26:2313–8.

815

816

Fig. 1. Phenotypic variation in male specimens collected along the *Ramphocelus flammigerus* hybrid zone in southwestern Colombia. Individuals 1-6 correspond to *R. flammigerus icteronotus* (yellow-rumped form) from the plains of the Pacific coast (sector 1; see Fig. 2). On the other extreme, individuals 11-14 correspond to *R. flammigerus flammigerus* (scarlet-rumped form) distributed towards the Cauca River Valley (sector 3). Individuals 7-10 are intermediates collected near the center of the hybrid zone (sector 2).
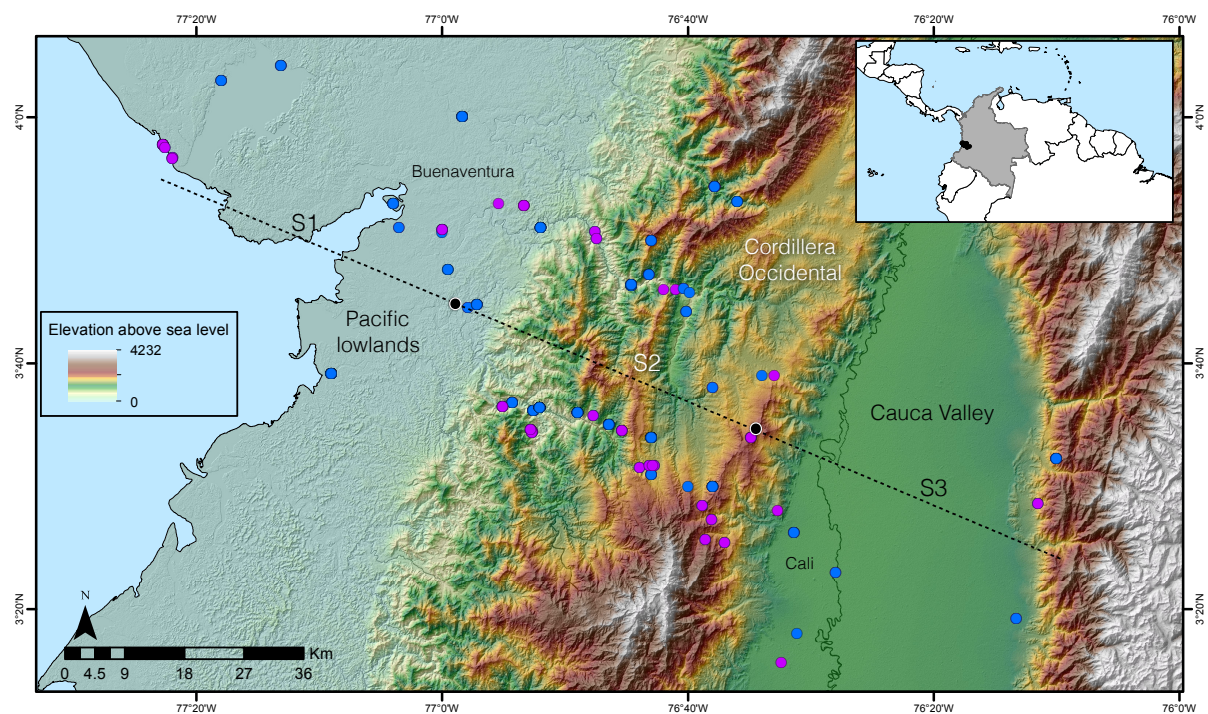
Fig. 2. Study transect encompassing the *Ramphocelus* hybrid zone from the Pacific lowlands to the eastern slope of the Cordillera Occidental of the Colombian Andes. Blue dots indicate collection sites of historical specimens and purple dots indicate collection sites of current specimens sampled for phenotypic/genetic variation; black lines correspond to municipality limits, with text indicating the location of the larger cities of Cali and Buenaventura. The extent of each of the three sectors we defined in the hybrid zone (S1, S2 and S3; see text) is indicated by black dots on the transect.

836
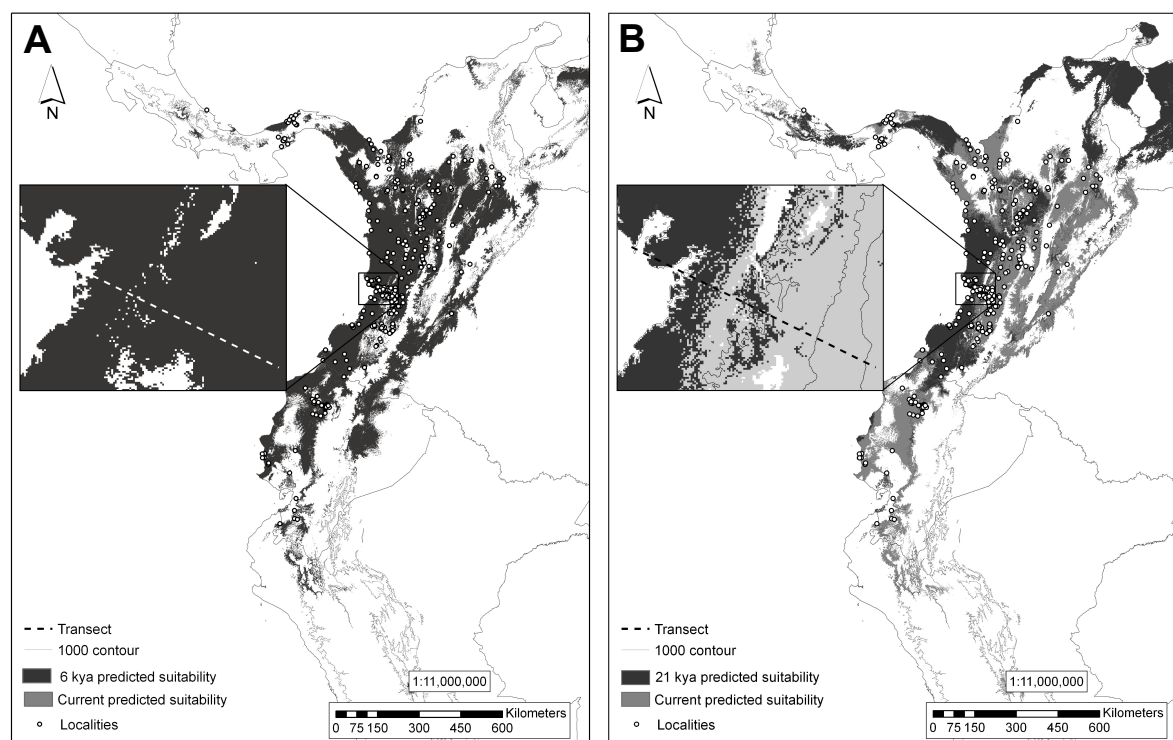
Fig. 3. Potential distributions of *R. flammigerus* predicted by MaxEnt using climatic data. Dark gray areas show suitable climatic conditions for the occurrence of *flammigerus* and *icteronotus* (A) 6,000 years ago and (B) 21,000 years ago (LGM). Light gray depicts climatically suitable areas for their occurrence at present. Note the smaller predicted range during the LGM and that the two forms likely did not exhibit a continuous range along the transect (dotted line) at that time, relative to the more extensive and continuous range modeled for 6,000 y.a. and under current conditions. Dots represent localities used to construct the models.

844
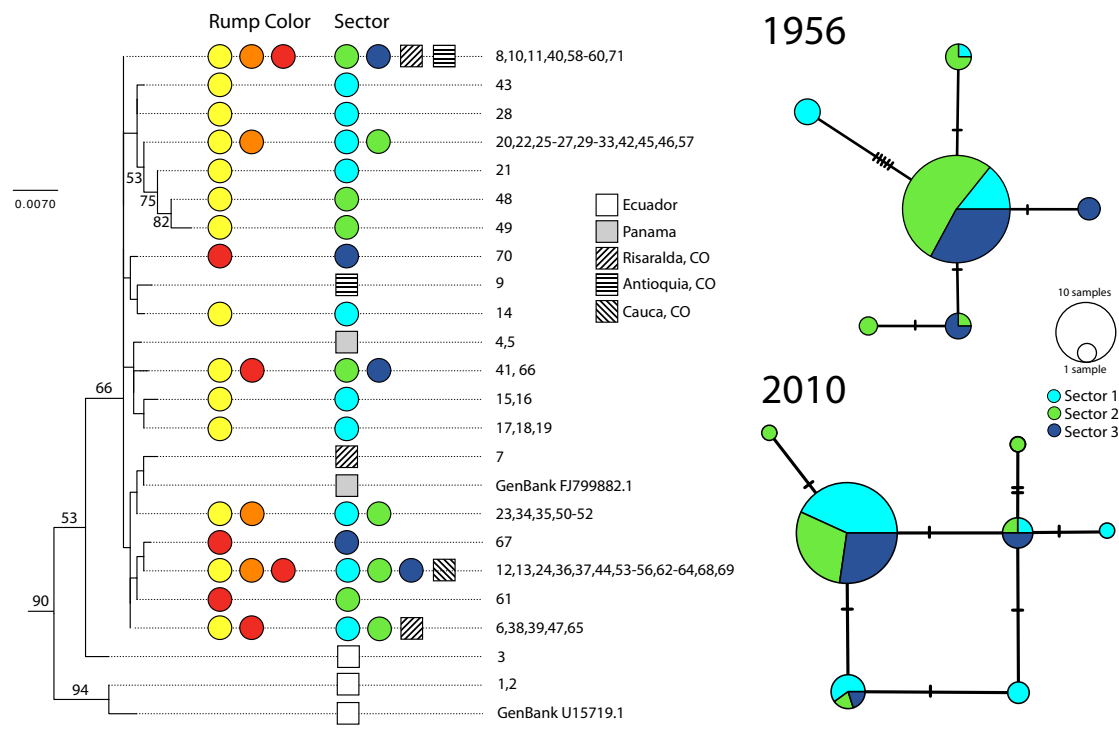
Fig. 4. Genealogical relationships of specimens of *R. flammigerus* showing limited geographic structuring and relatively low levels of sequence divergence among haplotypes. The phylogenetic tree on the left depicts relationships among nearly complete sequences of the cytochrome *b* gene obtained for individuals from the hybrid zone and other localitites inferred using maximum-likelihood (outgroups not shown); bootstrap values on nodes are shown when ≥ 50%. Colored circles indicate a qualitative assessment of the rump color (yellow, orange and red as in individuals 1-6, 7-10 and 11-14 in Fig. 1, respectively) and location in the hybrid zone (cyan, sector 1; green, sector 2; dark blue, sector 3) of individuals from the study transect exhibiting each haplotype. The numbers correspond to specimen identifications in Table S1; all numbers refer to specimens from the hybrid-zone transect unless otherwise noted. Localities outside the transect in different provinces of Colombia (CO), Ecuador, and Panama are indicated with squares. Haplotype networks on the right focused on specimens from the hybrid zone show that genetic variation in 210 bp of the cytochrome *b* gene was not clearly consistent with position of individuals along the hybrid zone in 1956 (top) or in the present (bottom), although analyses of molecular variance suggest differences in patterns of genetic structure across time periods (see text); circle sizes are proportional to the number of individuals sharing each haplotype.

863
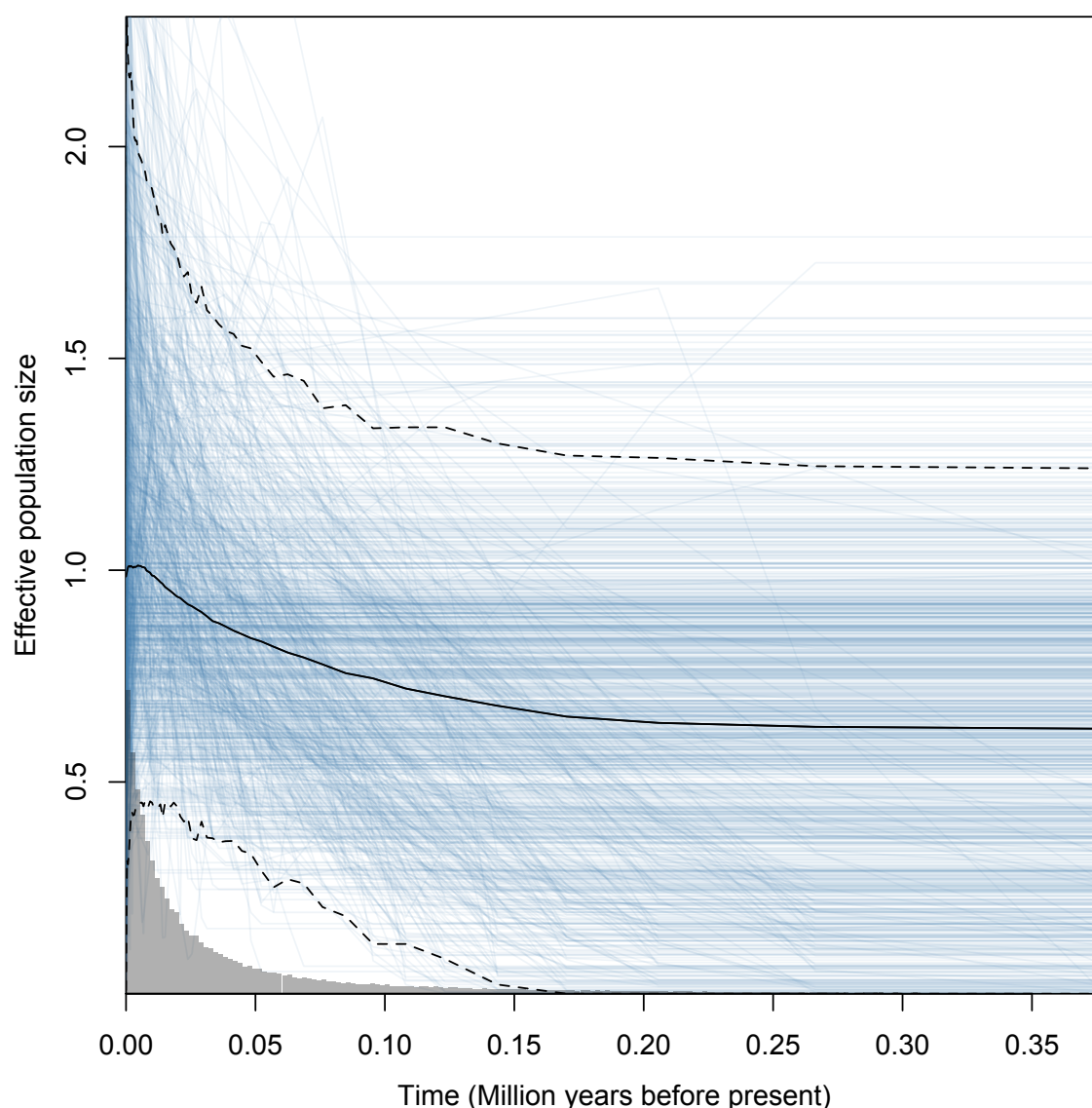
Fig. 5. Estimates of population sizes over the last 400,000 years obtained using the extended Bayesian skyline plot method applied to cytochrome *b* sequence data suggest demographic expansion towards the present in *R. flammigerus*. Median and credibility interval values are shown in black solid line and dashed lines, respectively. Blue lines correspond to 1000 genealogies used to estimate the 95% highest posterior density of population sizes. Bars in the histogram are proportional to the number of genealogies with values in the specific time interval.

870

871
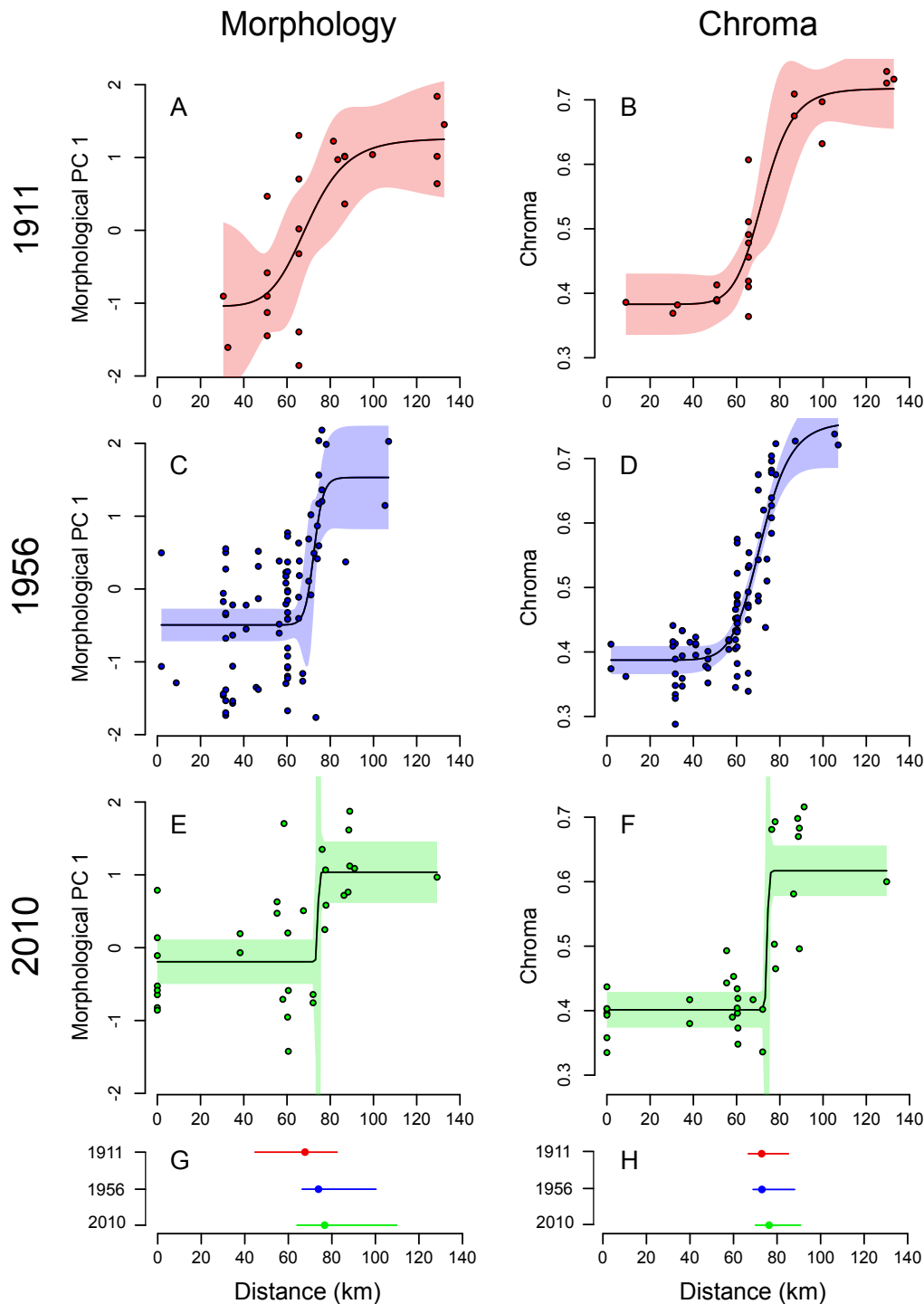
Fig. 6. Variation in morphology and coloration of males over c. 130 km across the *Ramphocelus* hybrid zone in historical and recent specimens. (A-F) Circles are values for individual specimens; dark lines are clines for traits and periods in which parameters were estimated using Hill functions, with shading indicating 95% confidence intervals around cline estimates. **(G, H)** Estimates of cline centers at each time period and their confidence limits estimated using bootstrap samples, revealing coincident eastward movement of the hybrid zone over time as indicated by both traits (colors as in A-F).
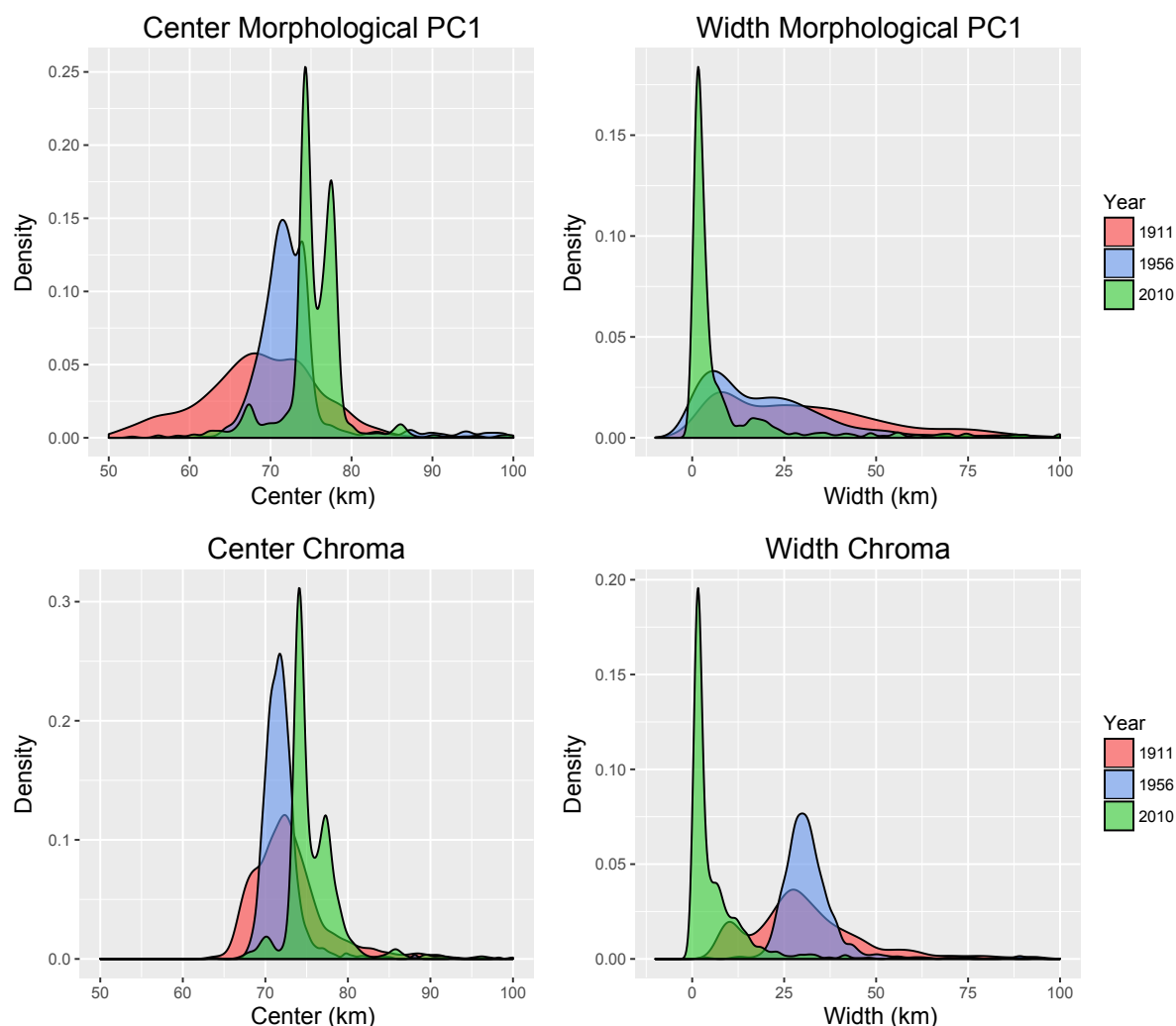
Figure 7. Probability density distibutions of cline center and cline width parameters estimated across 1,000 bootstrap samples of specimens for the 1911 (red), 1956 (blue), and 2010 (green) time periods. Both morphological PC1 and chroma show a shift in cline center and a reduction of cline width over time.

888 **Table 1. Population genetic structure in historical and recent specimens.** Results are shown for
889 analyses of molecular variance (AMOVA) based on DNA sequences of the cytochrome b
890 mitochondrial gene for 87 individuals collected in 1956 and 58 individuals collected in 2010.

	1956	2010
FST		
Among localities among sectors	0.26220	0.19669
P-value	0.08504	0.15445
Variance components	0.34011	0.26911
% variation	73.78	80.33
FSC		
Among populations within sectors	0.07916	-0.02096
P-value	0.05181	0.24047
Variance components	0.02924	-0.00552
% variation	6.34	-1.65
FCT		
Among sectors	0.19878	0.21318
P-value	0.01173	0.11144
Variance components	0.09163	0.07141
% variation	19.88	21.32

891

892

32

893 **Table 2. Validation of Hill-function methods as tools to estimate cline parameters.** For each of

894 seven genetic loci sampled across a *Manacus* hybrid zone in Panama, values of cline center and width

895 estimated using Hill functions are similar to point estimates of these parameters obtained by a previous

896 study [65] using cline-fitting algorithms HZAR (grey cells) and Analyse (white cells).

Locus	Center (c)		Width (w)	
	Hill Values	**HZAR/Analyse values**	**Hill Values**	**HZAR/Analyse values**
ada.A	155.35726	170.9 (109.9-201.2)	140.048	263.1 (96.2-630.0)
		171 (108.7-200.1)		262.5 (110.0-856.4)
ak2.A	208.796978	208.7 (207.2–210.2)	9.962	9.5 (0.1–15.7)
		208.6 (207.3–210.2)		9.9 (0.9–15.3)
pgm2.B	206.4	206.4 (201.3–209.9)	8.9027	7.7 (0.07–12.2)
		206.5 (201.5–209.5)		7.7 (0.5–12.0)
grs.B	221.959563	209.9 (201.7–224.5)	43.28	5.7 (0.009–44.3)
		209.9 (202.1–223.1)		2.9 (0.2–37.9)
l5.B	208.147795	208.1 (204.7–210.0)	11.378	8.1 (2.9–18.4)
		208.2 (206.2–208.4)		10.4 (7.2–14.4)
pscn3.B	208.565929	209.7 (206.6–210.0)	7.946	1.4 (0.1–15.5)
		209.4 (206.7–209.9)		2.8 (0.6–15.4)
mtDNA.B	208.208416	208 (206.0–210.8)	12.746	11.2 (6.8–19.5)
		208.3 (206.4–210.3)		11.1 (6.9–19.0)

897

898

899

900

901

902

903

904

905

906

907

908

909

910

911

912

Table 3. Cline parameters estimated for morphological and coloration data in historical and recent specimens. The table shows mean values of cline centers and widths obtained from bootstrap samples of morphological variation (PC1) and plumage chroma for each time period based on data for male specimens. Values in parentheses correspond to the 95% confidence intervals. All values are given in kilometers, with cline centers measured as the distance along the transect from the Pacific coast extreme (Fig. 2). No confidence limit is given for the width parameter in morphology in 2010 because bootstrapping produced unrealistic parameters (see text).

920

		Center (c)	Width (w)
1911	Chroma	72.92	31.48
		(66.74-85.27)	(8.78-78.69)
	PC 1	67.67	41.75
		(44.69-82.44)	(3.61-165.4)
1956	Chroma	73.04	32.37
		(68.96-88.07)	(21.14-60.48)
	PC 1	73.85	21.97
		(66.32-100.3)	(0.84-86.43)
2010	Chroma	76.33	6.71
		(70.02-90.8)	0.75-34.07
	PC 1	76.69	33.12
		(63.95-109.84)	-

921

922

923 **Table 4.** Results of post-hoc ANOVA comparing of clines center (c) and widths (w) among three time

924 periods for morphological (PC1) and plumage coloration (chroma) data using the bootstrap

925 distributions of parameters infered from Hill functions. Numbers correspond to *P* values of Tukey's

926 test, with those in bold indicating significant differences between periods.

927

				Center (c)				
		Chroma				*PC 1*		
Year	1911	1956	2010	Year	1911	1956	20:
1911	-	0.92	**0.00**	1911	-	**0.00**	**0.0**
1956		-	**0.00**	1956		-	**0.0**
2010			-	2010			-
				Width (w)				
		Chroma				*PC 1*		
Year	1911	1956	2010	Year	1911	1956	20:
1911	-	0.30	**0.00**	1911	-	**0.01**	0.3
1956		-	**0.00**	1956		-	0.2
2010			-	2010			-

928

929

930

931

932

933

934

935

936

937

938

939

940

941

942

35

943

944
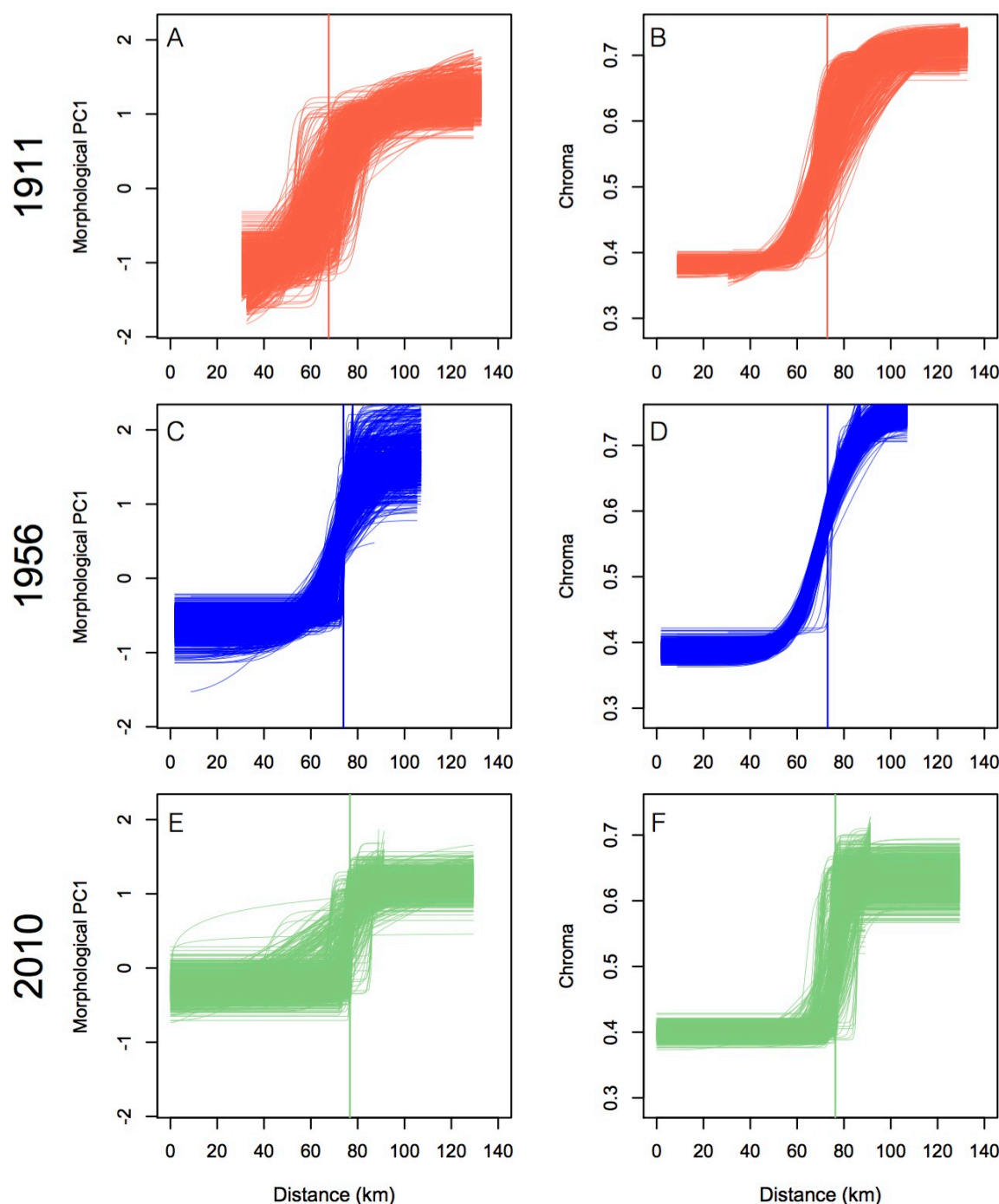
Figure S1. Clines for morphological and plumage data estimated across 1,000 bootstrap samples. The vertical line in each plot corresponds to the mean value of cline centers for the 1911 (A,B), 1956 (C,D) and 2010 (E,F) periods.

948

949
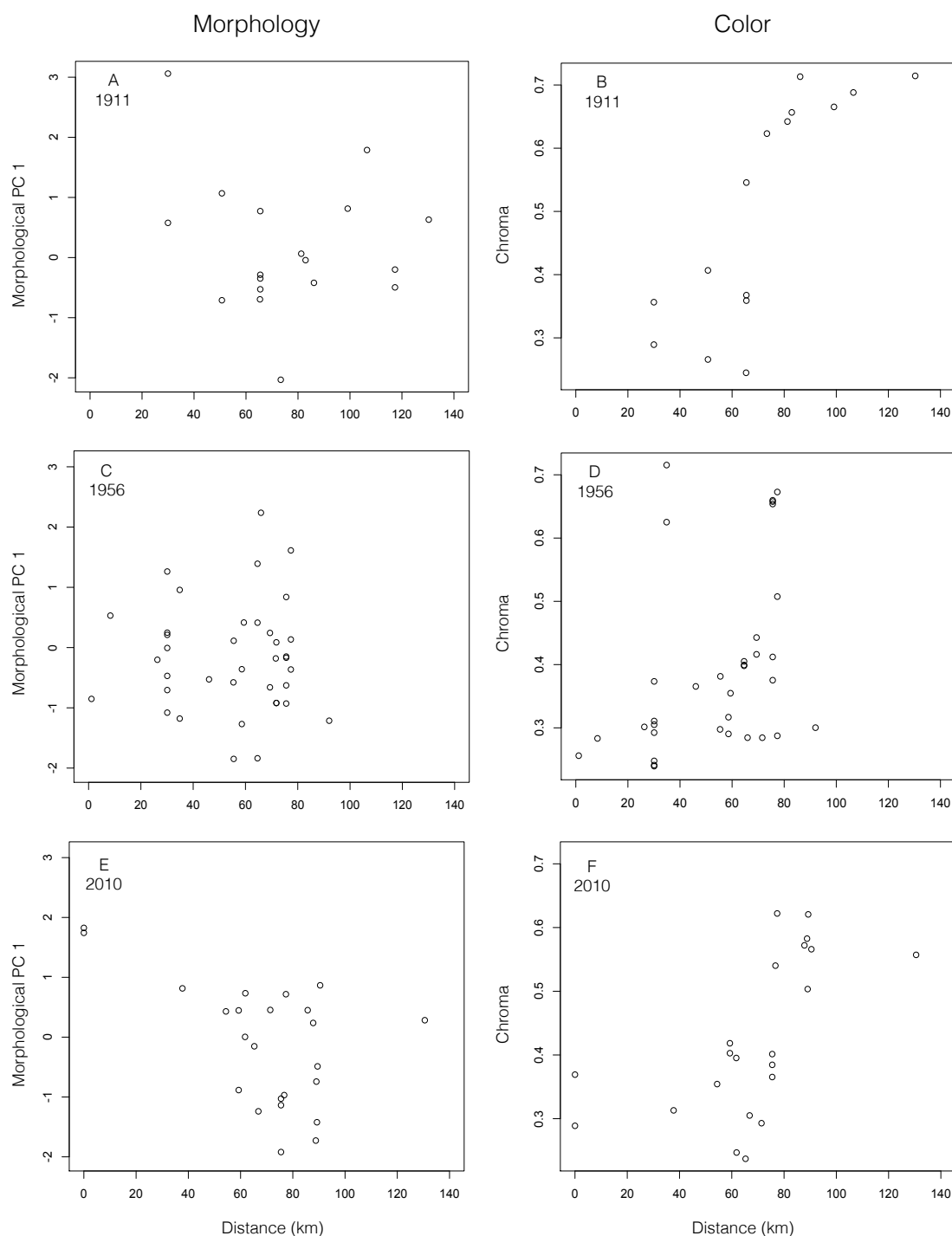
Figure S2. Variation in morphology (morphological PC1) and plumage chroma in female specimens across the *Ramphocelus flammigerus* hybrid zone in southwestern Colombia. Data are shown separately for historical specimens (A,B: 1911; C,D: 1956) and recent specimens (E,F: 2010).

37

Table S1 Information on the samples of *Ramphocelus flammigerus* included in the study, including identification number (ID), locality, museum catalogue number, geographical coordinates, and GenBank accession numbers for cytb sequences. Museum acronyms are as follows: LSUMZ: Louisiana State University Museum of Natural Science; ANDES-O: Museo de Historia Natural, Universidad de los Andes CUMV: Cornell University Museum of Vertebrates, Cornell University.

| Id	Locality	Catalogue No.	Latitude	Longitude	Accession No.
1	Ecuador, Esmeraldas Province El Placer	LSUMZ B-12014	0.867	-78.550	KR869689
2	Ecuador, Esmeraldas Province, El Placer	LSUMZ B-12017	0.867	-78.550	KR869688
3	Ecuador, Pichincha Province 5 km	LSUMZ B-35022	0.017	-78.883	KR869690
4	Panamá, Colon Province: Achiote Road	LSUMZ B-28758	9.223	-80.019	KR869691
5	Panamá, Darien Province	LSUMZ B-52947	8.083	-77.883	KR869692
6	Colombia, Risaralda, Pueblo Rico	ANDES-O AMR106	5.231	-76.084	KR869693
7	Colombia, Risaralda, Pueblo Rico	ANDES-O AMR107	5.231	-76.084	KR869694
8	Colombia, Risaralda, Pueblo Rico	ANDES-O NGP93	5.235	-76.085	KR869695
9	Colombia, Antioquia, San Roque	ANDES-O AMR118	6.384	-74.992	KR869696
10	Colombia, Antioquia, Cocorná	ANDES-O AMR55	6.027	-75.144	KR869697
11	Colombia, Antioquia, Cocorná	ANDES-O AMR56	6.027	-75.144	KR869698
12	Colombia, Cauca, Popayán	ANDES-O AMR83	2.477	-76.575	KR869700
13	Colombia, Cauca, Popayán	ANDES-O AMR84	2.477	-76.575	KR869699
14	Colombia, Valle del Cauca, Buenaventura, La Barra	ANDES-O NGP101	3.963	-77.379	KR817417
15	Colombia, Valle del Cauca, Buenaventura, La Barra	ANDES-O NGP99	3.963	-77.379	KR817418
16	Colombia, Valle del Cauca, Buenaventura, La Barra	ANDES-O AFR29	3.963	-77.379	KR817419

Id	Locality	Catalogue No.	Latitude	Longitude	Accession No.
17	Colombia, Valle del Cauca, Ladrilleros, Vía la Barra	ANDES-O AMR39	3.946	-77.366	KR817423
18	Colombia, Valle del Cauca, Buenaventura, La Barra	ANDES-O AMR86	3.963	-77.379	KR817420
19	Colombia, Valle del Cauca, Buenaventura, Ladrilleros	ANDES-O AMR40	3.944	-77.366	KR817422
20	Colombia, Valle del Cauca, B/tura, La Barra	ANDES-O AMR112	3.963	-77.379	KR817459
21	Colombia, Valle del Cauca, Buenaventura, La Barra	ANDES-O AMR111	3.959	-77.376	KR817428
22	Colombia, Valle del Cauca, Buenaventura, La Barra	ANDES-O AMR87	3.964	-77.379	KR817473
23	Colombia, Valle del Cauca, Buenaventura, Ladrilleros	ANDES-O AMR41	3.946	-77.366	KR817440
24	Colombia, Valle del Cauca, Buenaventura	ANDES-O AMR105	3.848	-77.000	KR817442
25	Colombia, Valle del Cauca, Buenaventura	ANDES-O AMR103	3.848	-77.000	KR817460
26	Colombia, Valle del Cauca, Buenaventura	ANDES-O AMR104	3.848	-77.000	KR817464
27	Colombia, Valle del Cauca, Dagua, El Placer	ANDES-O AMR95	3.591	-76.814	KR817466
28	Colombia, Valle del Cauca, Dagua, Alto Anchicayá	ANDES-O AMR47	3.575	-76.855	KR817462
29	Colombia, Valle del Cauca, Dagua, Alto Anchicayá	ANDES-O AMR69	3.573	-76.879	KR817472
30	Colombia, Valle del Cauca, Dagua, Bajo	ANDES-O NGP28	3.609	-76.918	KR817463
31	Colombia, Valle del Cauca, Dagua, Alto Anchicayá	ANDES-O AMR68	3.535	-76.871	KR817471
32	Colombia, Valle del Cauca, Dagua, Bajo Anchicayá	ANDES-O AMR64	3.609	-76.918	KR817470
33	Colombia, Valle del Cauca, Dagua, Alto Anchicayá	ANDES-O AMR45	3.574	-76.878	KR817474
34	Colombia, Valle del Cauca, Dagua, Alto Anchicayá	ANDES-O NGP27	3.576	-76.880	KR817435
35	Colombia, Valle del Cauca, Dagua, Alto Anchicayá	ANDES-O AMR66	3.576	-76.880	KR817439
36	Colombia, Valle del Cauca, Dagua, Alto Anchicayá	ANDES-O NGP30	3.576	-76.880	KR817445

Id	Locality	Catalogue No.	Latitude	Longitude	Accession No.
37	Colombia, Valle del Cauca, Dagua, Bajo Anchicayá	ANDES-O AMR65	3.609	-76.918	KR817446
38	Colombia, Valle del Cauca, Buenaventura, Los Tubos	ANDES-O AMR42	3.845	-76.793	KR817433
39	Colombia, Valle del Cauca, Buenaventura, La Delfina	ANDES-O AMR43	3.836	-76.791	KR817432
40	Colombia, Valle del Cauca, Dagua, Queremal	ANDES-O AMR102	3.595	-76.795	KR817455
41	Colombia, Valle del Cauca, Dagua, La Elsa	ANDES-O AMR98	3.576	-76.756	KR817424
42	Colombia, Valle del Cauca, Dagua, Alto Anchicayá	ANDES-O NGP29	3.573	-76.878	KR817465
43	Colombia, Valle del Cauca, Dagua, Alto Anchicayá	ANDES-O AMR63	3.576	-76.879	KR817430
44	Colombia, Valle del Cauca, Dagua, La Elsa	ANDES-O AMR97	3.576	-76.756	KR817443
45	Colombia, Valle del Cauca, Dagua, Alto Anchicayá	ANDES-O AMR48	3.575	-76.879	KR817468
46	Colombia, Valle del Cauca, Dagua, Alto Anchicayá	ANDES-O AMR49	3.574	-76.878	KR817469
47	Colombia, Valle del Cauca, Dagua, Alto Anchicayá	ANDES-O AMR46	3.575	-76.879	KR817431
48	Colombia, Valle del Cauca, Dagua, Queremal	ANDES-O AMR70	3.528	-76.719	KR817421
49	Colombia, Valle del Cauca, Dagua, Queremal	ANDES-O AMR74	3.527	-76.713	KR817426
50	Colombia, Valle del Cauca, Dagua, Queremal	ANDES-O AMR78	3.526	-76.733	KR817436
51	Colombia, Valle del Cauca, Dagua, Queremal	ANDES-O AMR75	3.526	-76.733	KR817437
52	Colombia, Valle del Cauca, Dagua, Queremal	ANDES-O AMR66	3.576	-76.880	KR817439
53	Colombia, Valle del Cauca, Dagua, Salado	ANDES-O AMR73	3.571	-76.697	KR817451
54	Colombia, Valle del Cauca, Dagua, Queremal	ANDES-O AMR76	3.526	-76.733	KR817447
55	Colombia, Valle del Cauca, Dagua, Queremal	ANDES-O AMR77	3.526	-76.733	KR817452
56	Colombia, Valle del Cauca, Dagua, Queremal	ANDES-O AMR72	3.526	-76.719	KR817444

Id	Locality	Catalogue No.	Latitude	Longitude	Accession No.
57	Colombia, Valle del Cauca, Cali, La Leonera	ANDES-O AMR85	3.455	-76.635	KR817467
58	Colombia, Valle del Cauca, La Cumbre	ANDES-O AMR37	3.575	-76.572	KR817457
59	Colombia, Valle del Cauca, La Cumbre, Chicoral	ANDES-O AMR36	3.566	-76.581	KR817458
60	Colombia, Valle del Cauca, Dagua, San Bernardo	ANDES-O AMR52	3.474	-76.647	KR817456
61	Colombia, Valle del Cauca, La Cumbre, Chicoral	ANDES-O AMR24	3.566	-76.581	KR817461
62	Colombia, Valle del Cauca, La Cumbre, Chicoral	ANDES-O AMR25	3.566	-76.581	KR817453
63	Colombia, Valle del Cauca, Cali, Peñas Blancas	ANDES-O AMR51	3.428	-76.643	KR817449
64	Colombia, Valle del Cauca, Cali, Peñas Blancas	ANDES-O AMR50	3.428	-76.643	KR817448
65	Colombia, Valle del Cauca, La Cumbre, Chicoral	ANDES-O AMR38	3.571	-76.575	KR817434
66	Colombia, Valle del Cauca, Cali, Andes	ANDES-O NGP102	3.422	-76.617	KR817425
67	Colombia, Valle del Cauca, Cali, Andes	ANDES-O AMR114	3.424	-76.617	KR817429
68	Colombia, Valle del Cauca, Cali, La Elvira	ANDES-O AMR53	3.526	-76.594	KR817450
69	Colombia, Valle del Cauca, Cali, Andes	ANDES-O AMR113	3.422	-76.617	KR817441
70	Colombia, Valle del Cauca, Palmira, La Buitrera	ANDES-O AMR115	3.476	-76.192	KR817427
71	Colombia, Valle del Cauca, Palmira, La Buitrera	ANDES-O AN006	3.471	-76.189	KR817454
72	Colombia, Valle del Cauca, Buenaventura	CUMV 27061	3.794	-76.993	KR817483
73	Colombia, Valle del Cauca, Buenaventura	CUMV 27062	3.794	-76.993	KR817542
74	Colombia, Valle del Cauca, Buenaventura	CUMV 27063	3.794	-76.993	KR817543
75	Colombia, Valle del Cauca, Buenaventura	CUMV 27064	3.794	-76.993	KR817544
76	Colombia, Valle del Cauca, Buenaventura	CUMV 27066	3.844	-77.000	KR817476

Id	Locality	Catalogue No.	Latitude	Longitude	Accession No.
77	Colombia, Valle del Cauca, Buenaventura	CUMV 27067	3.794	-76.993	KR817477
78	Colombia, Valle del Cauca, Buenaventura, Río Anchicaya	CUMV 27037	3.614	-76.905	KR817528
79	Colombia, Valle del Cauca, Buenaventura, Río Anchicaya	CUMV 27038	3.614	-76.905	KR817529
80	Colombia, Valle del Cauca, Buenaventura, Río Anchicaya	CUMV 27039	3.614	-76.905	KR817475
81	Colombia, Valle del Cauca, Buenaventura, Río Anchicaya	CUMV 27040	3.614	-76.905	KR817530
82	Colombia, Valle del Cauca, Buenaventura, Río Anchicaya	CUMV 27041	3.614	-76.905	KR817531
83	Colombia, Valle del Cauca, Buenaventura, Río Anchicaya	CUMV 27042	3.614	-76.905	KR817491
84	Colombia, Valle del Cauca, Buenaventura, Zabaletas	CUMV 27069	3.745	-76.953	KR817478
85	Colombia, Valle del Cauca, Buenaventura, Zabaletas	CUMV 27072	3.745	-76.953	KR817546
86	Colombia, Valle del Cauca, Buenaventura, Zabaletas	CUMV 27073	3.745	-76.953	KR817547
87	Colombia, Valle del Cauca, Buenaventura, El Placer	CUMV 27013	3.606	-76.868	KR817513
88	Colombia, Valle del Cauca, Buenaventura, El Placer	CUMV 27015	3.606	-76.868	KR817514
89	Colombia, Valle del Cauca, Buenaventura, El Placer	CUMV 27016	3.606	-76.868	KR817515
90	Colombia, Valle del Cauca, Buenaventura, El Placer	CUMV 27017	3.606	-76.868	KR817479
91	Colombia, Valle del Cauca, Buenaventura, El Placer	CUMV 27018	3.606	-76.868	KR817480
92	Colombia, Valle del Cauca, Buenaventura, El Placer	CUMV 27020	3.606	-76.868	KR817516
93	Colombia, Valle del Cauca, Buenaventura, El Placer	CUMV 27024	3.606	-76.868	KR817489
94	Colombia, Valle del Cauca, Buenaventura, El Placer	CUMV 27022	3.606	-76.868	KR817518
95	Colombia, Valle del Cauca, Buenaventura, El Placer	CUMV 27024	3.606	-76.868	KR817489
96	Colombia, Valle del Cauca, Buenaventura, El Placer	CUMV 27026	3.606	-76.868	KR817519

Id	Locality	Catalogue No.	Latitude	Longitude	Accession No.
97	Colombia, Valle del Cauca, Buenaventura, El Placer	CUMV 27027	3.606	-76.868	KR817520
98	Colombia, Valle del Cauca, Buenaventura, El Placer	CUMV 27028	3.606	-76.868	KR817481
99	Colombia, Valle del Cauca, Buenaventura, El Placer	CUMV 27029	3.606	-76.868	KR817495
100	Colombia, Valle del Cauca, Buenaventura, El Placer	CUMV 27030	3.606	-76.868	KR817521
101	Colombia, Valle del Cauca, Buenaventura, El Placer	CUMV 27031	3.606	-76.868	KR817522
102	Colombia, Valle del Cauca, Buenaventura, El Placer	CUMV 27032	3.606	-76.868	KR817523
103	Colombia, Valle del Cauca, Buenaventura, El Placer	CUMV 27033	3.606	-76.868	KR817524
104	Colombia, Valle del Cauca, Buenaventura, El Placer	CUMV 27034	3.606	-76.868	KR817525
105	Colombia, Valle del Cauca, Buenaventura, El Placer	CUMV 27035	3.606	-76.868	KR817526
106	Colombia, Valle del Cauca, Buenaventura, El Placer	CUMV 27036	3.606	-76.868	KR817527
107	Colombia, Valle del Cauca, Dagua, Queremal	CUMV 27044	3.517	-76.717	KR817488
108	Colombia, Valle del Cauca, Dagua, La Elsa	CUMV 27046	3.583	-76.774	KR817494
109	Colombia, Valle del Cauca, Buenaventura, Río Anchicaya	CUMV 27040	3.614	-76.905	KR817530
110	Colombia, Valle del Cauca, Dagua, La Elsa	CUMV 27049	3.583	-76.774	KR817532
111	Colombia, Valle del Cauca, Dagua, La Elsa	CUMV 27050	3.583	-76.774	KR817533
112	Colombia, Valle del Cauca, Dagua, La Elsa	CUMV 27051	3.583	-76.774	KR817534
113	Colombia, Valle del Cauca, Dagua, La Elsa	CUMV 27052	3.583	-76.774	KR817535
114	Colombia, Valle del Cauca, Dagua, La Elsa	CUMV 27053	3.583	-76.774	KR817536
115	Colombia, Valle del Cauca, Dagua, La Elsa	CUMV 27055	3.583	-76.774	KR817537
116	Colombia, Valle del Cauca, Dagua, La Elsa	CUMV 27056	3.583	-76.774	KR817538

Id	Locality	Catalogue No.	Latitude	Longitude	Accession No.
117	Colombia, Valle del Cauca, Dagua, La Elsa	CUMV 27057	3.583	-76.774	KR817539
118	Colombia, Valle del Cauca, Dagua, La Elsa	CUMV 27058	3.583	-76.774	KR817482
119	Colombia, Valle del Cauca, Dagua, La Elsa	CUMV 27059	3.583	-76.774	KR817540
120	Colombia, Valle del Cauca, Dagua, La Elsa	CUMV 27060	3.583	-76.774	KR817541
121	Colombia, Valle del Cauca, Dagua, Rio Blanco	CUMV 27068	3.600	-76.817	KR817545
122	Colombia, Valle del Cauca, Dagua, Rio Blanco	CUMV 27074	3.600	-76.817	KR817548
123	Colombia, Valle del Cauca, Dagua, Rio Blanco	CUMV 27076	3.600	-76.817	KR817490
124	Colombia, Valle del Cauca, Dagua, Rio Blanco	CUMV 27078	3.600	-76.817	KR817549
125	Colombia, Valle del Cauca, Dagua, Rio Blanco	CUMV 27079	3.600	-76.817	KR817550
126	Colombia, Valle del Cauca, Dagua, Rio Blanco	CUMV 27082	3.600	-76.817	KR817551
127	Colombia, Valle del Cauca, Dagua, Rio Blanco	CUMV 27083	3.600	-76.817	KR817552
128	Colombia, Valle del Cauca, Dagua, Rio Blanco	CUMV 27084	3.600	-76.817	KR817553
129	Colombia, Valle del Cauca, Dagua, Salado	CUMV 26992	3.567	-76.717	KR817558
130	Colombia, Valle del Cauca, Dagua, Salado	CUMV 26993	3.567	-76.717	KR817502
131	Colombia, Valle del Cauca, Dagua, Salado	CUMV 26994	3.567	-76.717	KR817557
132	Colombia, Valle del Cauca, Dagua, Salado	CUMV 26995	3.567	-76.717	KR817492
133	Colombia, Valle del Cauca, Dagua, Salado	CUMV 26996	3.567	-76.717	KR817503
134	Colombia, Valle del Cauca, Dagua, Salado	CUMV 26997	3.567	-76.717	KR817497
135	Colombia, Valle del Cauca, Dagua, Salado	CUMV 26998	3.567	-76.717	KR817504
136	Colombia, Valle del Cauca, Dagua, Salado	CUMV 26999	3.567	-76.717	KR817505

Id	Locality	Catalogue No.	Latitude	Longitude	Accession No.
137	Colombia, Valle del Cauca, Dagua, Salado	CUMV 27000	3.567	-76.717	KR817506
138	Colombia, Valle del Cauca, Dagua, Salado	CUMV 27001	3.567	-76.717	KR817507
139	Colombia, Valle del Cauca, Dagua, Salado	CUMV 27002	3.567	-76.717	KR817484
140	Colombia, Valle del Cauca, Dagua, Salado	CUMV 27003	3.567	-76.717	KR817508
141	Colombia, Valle del Cauca, Dagua, Salado	CUMV 27004	3.567	-76.717	KR817509
142	Colombia, Valle del Cauca, Dagua, Salado	CUMV 27005	3.567	-76.717	KR817510
143	Colombia, Valle del Cauca, Dagua, Salado	CUMV 27006	3.567	-76.717	KR817493
144	Colombia, Valle del Cauca, Dagua, Salado	CUMV 27007	3.567	-76.717	KR817485
145	Colombia, Valle del Cauca, Dagua, Salado	CUMV 27008	3.567	-76.717	KR817511
146	Colombia, Valle del Cauca, Dagua, Salado	CUMV 27010	3.567	-76.717	KR817487
147	Colombia, Valle del Cauca, Dagua, Salado	CUMV 27011	3.567	-76.717	KR817512
148	Colombia, Valle del Cauca, Dagua, Salado	CUMV 27012	3.567	-76.717	KR817486
149	Colombia, Valle del Cauca, Dagua, Queremal	CUMV 27045	3.517	-76.717	KR817496
150	Colombia, Valle del Cauca, La Cumbre, San Antonio	CUMV 22956	3.500	-76.633	KR817498
151	Colombia, Valle del Cauca, La Cumbre, San Antonio	CUMV 22958	3.500	-76.633	KR817499
152	Colombia, Valle del Cauca, Palmira, La Manuelita	CUMV 22959	3.583	-76.283	KR817500
153	Colombia, Valle del Cauca, Palmira, Miraflores	CUMV 22961	3.578	-76.434	KR817501
154	Colombia, Valle del Cauca, Tulua, La Paila	CUMV 27086	4.319	-76.072	KR817554
155	Colombia, Valle del Cauca, Jamundi, La Olga	CUMV 27087	3.299	-76.519	KR817555
156	Colombia, Valle del Cauca, Buga, La Habana	CUMV 27088	3.881	-76.191	KR817556